Evolutionary History of Voltage-Gated Sodium Channels

Atsuo Nishino and Yasushi Okamura

Contents

Abstract

Every cell within living organisms actively maintains an intracellular Na^+ concentration that is 10–12 times lower than the extracellular concentration. The cells then utilize this transmembrane Na^+ concentration gradient as a driving force to produce electrical signals, sometimes in the form of action potentials. The protein family comprising voltage-gated sodium channels (Na_Vs) is essential for such signaling and enables cells to change their status in a regenerative manner and to rapidly communicate with one another. Na_Vs were first predicted in squid and were later identified through molecular biology in the electric eel. Since then, these proteins have been discovered in organisms ranging from bacteria to humans. Recent research has succeeded in decoding the amino acid sequences of a wide variety of Na_V family members, as well as the three-dimensional structures of some. These studies and others have uncovered several of the major steps in the functional and structural transition of Na_V proteins that has occurred along the course of the evolutionary history of organisms. Here we present an overview of the molecular evolutionary innovations that established

A. Nishino (✉)
Department of Biology, Faculty of Agriculture and Life Science, Hirosaki University, Hirosaki, Aomori, Japan
e-mail: anishino@hirosaki-u.ac.jp

Y. Okamura
Integrative Physiology, Graduate School of Medicine, Osaka University, Suita, Osaka, Japan

present-day Na_V α subunits and discuss their contribution to the evolutionary changes in animal bodies.

1 Introduction

Hodgkin and Huxley in the 1940s–1950s suggested the presence of pores that enabled selective permeation of Na^+ and K^+ ions that was dependent on membrane depolarization and shaped the action potentials (APs). The Na^+-based APs were first recorded from the giant axons of the squid *Loligo* (e.g., Hodgkin and Huxley 1945, 1952). Since then, we have come to recognize voltage-gated Na^+ channels (Na_Vs) as a core element of the nerve impulse that supports essentially all brain function. William A. Catterall and colleagues succeeded in purifying the biochemical component of Na_Vs from rat brains (e.g., Beneski and Catterall 1980; Hartshorne and Catterall 1981; Hartshorne et al. 1985). Noda et al. (1984) isolated a cDNA encoding the pore-forming α subunit of the Na_V from the electric eel, *Electrophorus*. Thereafter, cDNAs for other Na_V α subunits have been cloned from mammals, other vertebrates, and invertebrates. In the fruit fly, *Drosophila melanogaster*, Na_V mutants called *para* were isolated, and the later studies have clearly linked the genotypes of the Na_V α subunit to cellular/whole body-level phenotypes (e.g., Loughney et al. 1989). Then the gene expression of Na_V in response to neural inductive signaling was shown to underlie development of membrane excitability in neurons in a simple chordate model, the ascidian *Halocynthia roretzi* (Okamura et al. 1994). In recent years, Na^+ channels derived from marine bacteria were utilized to increase our understanding of the structural and biophysical basis of Na^+ ion selectivity and voltage dependence (e.g., Payandeh and Minor 2015; Catterall and Zheng 2015). And very recently, genes from the cockroach *Periplaneta* and from *Electrophorus* were utilized to finally resolve the 3D structures of metazoan Na_Vs (Shen et al. 2017; Yan et al. 2017). This brief history of Na^+ channel research reflects the long, but cooperative, struggle to uncover the essence of nature (membrane excitability here) through the use of appropriate biological materials at appropriate times, seemingly making manifest August Krogh's Principle (Krebs 1975).

The aforementioned analyses were performed using Na_Vs from a variety of animal species and demonstrated that the amino acid sequences of the channel proteins have changed to varying degrees and have incorporated innovations in accordance with the evolution of the animals harboring the channels. Given the well-known statement by T. Dobzhansky that nothing in biology makes sense except in the light of evolution, the diversity of Na_Vs provides us with rich insight. Like other gene families, the Na_V gene family grew through gene duplication, sequence changes, and natural selection. These processes now enable animals to utilize similar but independent Na_Vs at different times during development and/or in specific cell types. In this review, we will outline mammalian, vertebrate, chordate, and metazoan Na_V α subunit diversity and the cell type-specific usage

of different isoforms, and we will introduce some of their molecular innovations that correlate with the evolution of animal lifestyles.

2 Structural Outlines of Voltage-Gated Sodium Channels

Metazoan Na$_V$s consist of four serially homologous sections, domains I-IV (Fig. 1). Each domain contains six α-helices constituting transmembrane regions S1-S6 linked to each other by extracellular or intracellular loops (Fig. 1a). As a result,
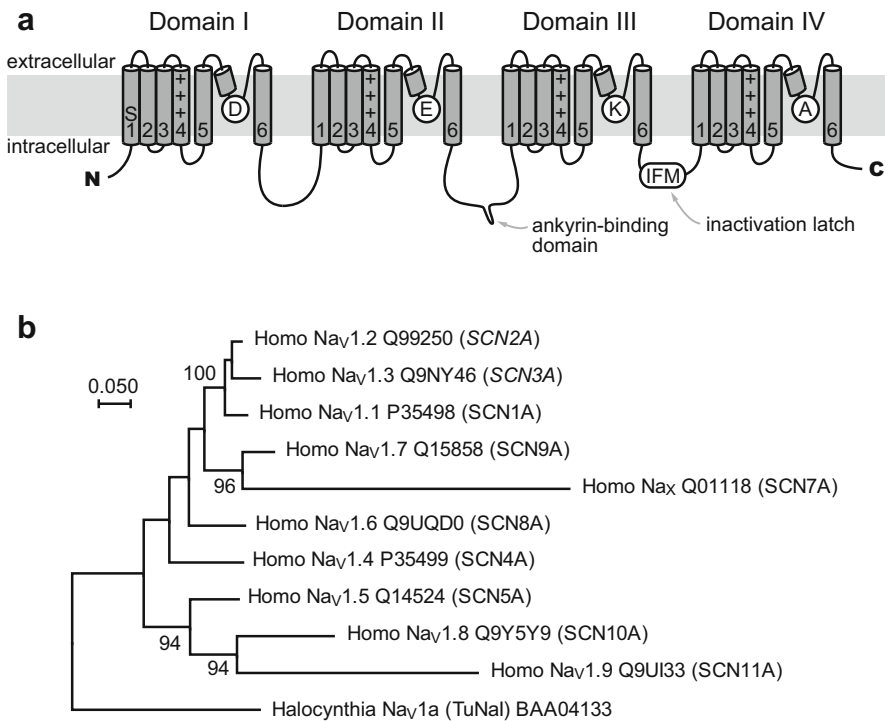
Fig. 1 Mammalian Na$_V$1 channel α subunits. (**a**) A schematic image of mammalian Na$_V$1 channels. Diagnostic characteristics of Na$_V$1s are indicated. Na$_V$1s have 24 transmembrane segments and are composed of serially homologous domains I–IV, each of which contains segments S1–S6. S4 segments harbor evenly spaced positively charged residues (+). Amino acids at the inner vertices of the loops between S5 and S6 pore-forming segments (P-loops) constitute an ion-selectivity filter. In the case of Na$_V$1s, the pore signature is Asp/Glu/Lys/Ala (D/E/K/A). The loop between domains II and III contains an ankyrin-binding motif sequence that is reportedly important to localize the Na$_V$1 channels to the axon initial segment and nodes of Ranvier. The sequence between domains III and IV functions as the inactivation latch (inactivation ball), the core of which is represented by the well-conserved Ile-Phe-Met (I-F-M) triplet. (**b**) A molecular phylogenetic tree of mammalian Na$_V$1 α subunits constructed by the maximum-likelihood method based on gap-free 1,372 amino acid positions using MEGA7. The sequence from the ascidian *Halocynthia* is used as the out-group. The bootstrap values over 80 are shown. The four groups (Na$_V$1.1/1.2/1.3/1.7, Na$_V$1.4, Na$_V$1.6, Na$_V$1.5/1.8/1.9) are recognized (see text and Table 1)

the full-length metazoan Na_V polypeptide contains a total of 24 transmembrane (TM) regions spanning about 2,000 amino acids. As was proposed for voltage-gated potassium channels (K_Vs), the S1-S4 segments in each domain function as a voltage sensor (e.g., Catterall 2000). In particular, the S4 segment, in which every third amino acid is a positive charged Arg or Lys residue, is considered essential for sensing membrane voltage. In the resting state, S4 is positioned closer to the intracellular side of the membrane. Upon membrane depolarization, S4 moves in an extracellular direction, and this change of conformation stimulates the channel gate to open (Catterall 2000; Shen et al. 2017; Yan et al. 2017). The S5 and S6 segments and the loop between them (P-loop) from each domain occupy a quarter of the central portion of the protein such that the four domains together form the wall, gate, and ion-selectivity filter of the channel (Catterall 2000; Shen et al. 2017).

Mammals, including humans, express nine Na_V isoforms (Na_V1.1 to Na_V1.9). In addition, a protein most similar to Na_V1.7, called Na_X, has also been identified in mammals (Fig. 1b, Table 1). Na_X does not exhibit ion permeability. Instead, it appears to function as a sensor of extracellular Na^+ ion and is now thought to be involved in ionic homeostasis in the body (Hiyama et al. 2002, 2004; Hiyama and Noda 2016). The cDNA sequences, predicted amino acid sequences, locations of the respective encoding genes (*SCN1A-11A*) on the chromosomes, spatiotemporal expression patterns, sensitivity to toxins [e.g., tetrodotoxin (TTX)], single-channel conductances, characteristics of inactivation, and biological functions of these isoforms have all been comprehensively analyzed (some characteristics of mammalian Na_Vs are listed in Table 1) (Goldin 2001; Catterall et al. 2005). For instance, mammalian Na_V1.1, 1.2, and 1.3 are encoded by *SCN1A*, *2A*, and *3A*, respectively, and these genes are tandemly arrayed within the genome (on the "q" arm of chromosome 2 in the case of humans) close to the *HoxD* gene cluster (Table 1). The primary structures of these isoforms are mutually similar, suggesting they emerged through relatively recent tandem gene duplications (Fig. 1b). This tandem cluster also includes the gene for Na_V1.7 (*SCN9A*), which is expressed in the peripheral nervous system (PNS), including the dorsal root ganglia (DRG)

Table 1 Mammalian voltage-gated sodium channel α subunits[a]

Channel name	Gene symbol	Adj. Hox cluster	Approx. TTX IC_{50}	Tissue to function
Na_V1.1	*SCN1A*	*HoxD*	10 nM	CNS
Na_V1.2	*SCN2A*	*HoxD*	10 nM	CNS
Na_V1.3	*SCN3A*	*HoxD*	10 nM	CNS
Na_V1.4	*SCN4A*	*HoxB*	10 nM	Skeletal muscle
Na_V1.5	*SCN5A*	*HoxA*	1–10 μM	Heart
Na_V1.6	*SCN8A*	*HoxC*	<10 nM	CNS
Na_V1.7	*SCN9A*	*HoxD*	10 nM	PNS
Na_V1.8	*SCN10A*	*HoxA*	>10 μM	PNS
Na_V1.9	*SCN11A*	*HoxA*	1 μM	PNS
Na_X	*SCN7A*	*HoxD*	–	CNS and others

[a]This table is modified from Goldin (2001)

(Sangameswaran et al. 1997; Toledo-Aral et al. 1997). The gene encoding Na_X (*SCN7A*) is also found in this cluster. $Na_V1.7$ and Na_X constitute a sister clade in the molecular phylogenetic tree, and the duplication of these two genes occurred in parallel with the splits of $Na_V1.1$, 1.2, and 1.3 (Fig. 1b) (Catterall et al. 2005). They commonly show high sensitivity to TTX, with IC_{50}s around 10 nM (summarized in Goldin 2001). In addition to the channels already mentioned, the central nervous system (CNS) expresses $Na_V1.6$, which exhibits characteristic persistent current and a large resurgent current, while the PNS expresses $Na_V1.8$ and 1.9. The heart expresses $Na_V1.5$, encoded by *SCN5A*, which clusters with *SCN10A* encoding $Na_V1.8$ and *SCN11A* encoding $Na_V1.9$, close to the *HoxA* cluster (Table 1). $Na_V1.8$ and 1.9 are also presumed to have emerged through tandem gene duplication that occurred after the two rounds of whole genome duplication in the ancestor of jawed vertebrates (see below) and share relatively slow activation kinetics (Fig. 1b) (Lai et al. 2004). Along with $Na_V1.5$, $Na_V1.8$ and 1.9 are relatively insensitive to TTX, with IC_{50} in the range of 1–10 μM or more (Gellens et al. 1992; Akopian et al. 1996; Tate et al. 1998). Skeletal muscles use $Na_V1.4$ for APs, and its gene, *SCN4A*, is not clustered with other Na_V genes and neighbors the *HoxB* cluster (Table 1). $Na_V1.4$ in skeletal muscle is as sensitive to TTX as Na_Vs in the CNS (NaV1.1–1.3, and 1.6).

All nine Na_Vs possess an activation gate that opens in response to membrane depolarization and an ion-selectivity filter that enables selective Na^+ permeation. The extracellular fluid around living cells generally contains a high concentration of Na^+, while the intracellular fluid has a lower Na^+ concentration. Na_V gating allows Na^+ to flow into the cell and depolarize the membrane, though the channel soon shuts through the process of inactivation. The inactivation function is one that the Na_V α subunits themselves possess and enables immediate repolarization of the membrane to sharpen the AP (Hodgkin and Huxley 1952). All known Na_Vs show some degree of inactivation, which is known to require the linker sequence between domains III and IV (Stühmer et al. 1989), a region called the "inactivation ball" or "inactivation latch" (Fig. 1a). The latch is modeled to fit into the open pore and block ion permeation (ball-and-chain model). Within the sequence of this linker, three consecutive hydrophobic amino acids, Ile-Phe-Met, are well shared by vertebrate Na_Vs and are totally conserved in all the human Na_V isoforms. This triplet, especially the central Phe residue, is essential for inactivation, and thus hydrophobic interaction between the latch and the open pore would be important (West et al. 1992; see also a recent revision to this model proposed from the structural study by Yan et al. 2017).

The P-loop between S5 and S6 in each of the four domains protrudes into the central canal of Na_Vs, and the inner vertices of the loops are thought to constitute the ion-selectivity filter (Heinemann et al. 1992; Shen et al. 2017). The residues for Na^+ ion selectivity in all mammalian Na_Vs are Asp from domain I, Glu from domain II, Lys from domain III, and Ala from domain IV (asymmetric D/E/K/A signature) (Fig. 1a). By contrast, most Ca_Vs, which have a similar 24-TM conformation, show a symmetric E/E/E/E pore signature (e.g., Hinemann et al. 1992). The 3–4 acidic residues behind the D/E/K/A signature residues (E/E/D/D in all

mammalian Na_Vs) form the "outer ring," which is also significant for positively charged ion permeability (Catterall 2000). The region around the signature residue in domain I is a definitive binding target for TTX (Noda et al. 1989). This selectivity filter is located midway through the canal, and the outer ring is a bit extracellular to the signature. On the intracellular side is a central cavity enclosed by charged residues, with the predicted activation gate composed of the S6 segments from domains I-IV aligned along the channel fenestration (Catterall 2000; Shen et al. 2017).

These structural features, including the 24-TM segments in the four serially homologous domains, the voltage-sensor domains, D/E/K/A selectivity filter, central cavity, activation gate, and inactivation latch are shared by all mammalian Na_V α subunits (e.g., Catterall 2000; Catterall et al. 2005).

3 Historical Origin of Voltage-Gated Sodium Channels and Their Related Proteins

The discovery of Na_Vs in bacteria ($BacNa_Vs$) confirmed that Na^+-permeable channel proteins gated in response to changes in membrane potential had already evolved in prokaryotes (Ren et al. 2001; Payandeh and Minor 2015). However, these $BacNa_Vs$ are composed of homotetrameric 6-TM subunits that contain compact S1-S6 segments (e.g., Payandeh and Minor 2015; Catterall and Zheng 2015). Because a $BacNa_V$ can be changed into Ca^{2+}-selective channel through simple mutation(s), it is thought that prokaryotes can also possess voltage-gated Ca^{2+} channels (Yue et al. 2002). In addition, the K_VAP channel, the first voltage-gated ion channel whose structure was resolved, is a K^+ channel from prokaryotic archaea (Jiang et al. 2003). It is thus evident that prokaryotes likely made use of a wide variety of voltage-gated, ion-specific 6-TM channels long before the emergence of eukaryotes. The 6-TM segments can be functionally divided into a voltage-sensing unit composed of segments S1-S4 and an ion channel pore domain corresponding to segments S5-S6, including the P-loop in between. Members of the prokaryotic KcsA-related channel and eukaryotic Kir channel families are composed of homotetrameric 2-TM helices, which are thought to represent units of the tetraradial pore domains (e.g., Bichet et al. 2003). The K2P channel family members show a tandem repeat of two pore domains, dimerization of which produces a channel pore of pseudotetrameric symmetry (e.g., Honoré 2007). Recent research has revealed that the voltage-sensor domain can also function independently of the pore domain. For instance, the recently identified voltage-sensing phosphatase (VSP) possesses S1-S4-like segments coupled to phosphatase domain that catalyze membrane phospholipid dephosphorylation in response to changes in membrane potential (Murata et al. 2005). It is also known that the primary structure of a voltage-dependent proton channel, H_V1/voltage-sensor-domain-only protein (VSOP), is comparable to segments S1-S4 of 6-TM voltage-gated ion channel subunits (Ramsey et al. 2006; Sasaki et al. 2006).

All of the prokaryotic voltage-gated ion channels identified so far are composed of homotetrameric 6-TM subunits. Eukaryotic voltage-gated K^+ channels

and Ca^{2+}-permeable Catsper channels are still tetrameric compositions of 6-TM subunits (Liebeskind et al. 2013). In addition to these, eukaryotes express larger voltage-gated ion channel proteins composed of 12-TM or 24-TM segments. The 12-TM channels are two-pore channels (TPCs), which are cation channels functioning within intracellular organelles such as endosomes and lysosomes (Calcraft et al. 2009). The 24-TM ion channel family includes not only Na_Vs but also L-, T-, and N/P/Q/R-type Ca_Vs (also called Ca_V1, Ca_V2, and Ca_V3, respectively) and cation leak channels (NALCN). It is thought that eukaryotic 24-TM channels harboring four-time serially homologous domains are derived from two rounds of tandem duplication of an original 6-TM factor. In fact, the amino acid sequences of domain I of the Na_V and Ca_V1, 2, and 3 channels are more similar to domain III than to II or IV, while the sequence in domain II is more like that of IV than domain I or III (Strong et al. 1993; Liebeskind et al. 2013). It is also known that the amino acid sequences of these four domains are closer to each other, and to those of the Catsper isoforms, than to the sequences of BacNa$_V$s or K_Vs. These relationships suggest eukaryotic 24-TM channels were not derived from duplication of a BacNa$_V$, but arose instead through two sequential rounds of duplication of a gene encoding a Catsper-like 6-TM protein; one duplication gave rise to a gene encoding 12-TM segments containing domain I and II, and a second tandem duplication established the present conformation composed of domains I-IV (Liebeskind et al. 2013). This process was significant in that the ion channel molecules got to be formed by a single polypeptide stretch, not by four identical subunits, which would facilitate accumulation of "asymmetric" mutations independently within domains I to IV to make the channel "pseudotetrameric." This implies that this process would potentiate future molecular evolutionary fine-tuning for specific functions – e.g., Na^+ selectivity, fast inactivation, anchoring, etc. (see below).

In addition to the channels mentioned to far, another 24-TM subfamily, Na_V2, has been identified in invertebrates, and its members have amino acid sequences similar to Na_V1, but exhibits a D/E/E/A pore signature (Salkoff et al. 1987; Sato and Matsumoto 1992; Nagahora et al. 2000; Zhou et al. 2004; Zakon 2012; Gur Barzilai et al. 2012; Moran et al. 2015). Later analyses proved that the members of this family are permeable to Ca^{2+}, and it has recently been proposed that this family be renamed Ca_V4 (Zhou et al. 2004; Gosselin-Badaroudine et al. 2016). It has also been reported that a mutant $Na_V1.2$ channel of rat giving a D/E/E/A pore signature is permeable not only to Na^+ but also to Ca^{2+} and K^+ and that the presence of a physiological concentration of Ca^{2+} in the extracellular fluid blocks permeation of Na^+ through the mutant channel (Heinemann et al. 1992). This nonselective permeation of cations is also observed in a cnidarian Na_V family channel having the D/E/E/A pore (called NvNa$_V$2.1), although it does not show the blockade by extracellular Ca^{2+} (Gur Barzilai et al. 2012). Given its sequence similarity to Na_V1 and its functional characteristics, we will refer to this subfamily as $Na_V2(Ca_V4)$ here.

The major diversification events of these families of 24-TM channels of animals, namely, evolutionary splits of the Na_V, Ca_V, and NALCN families, predate the origin of metazoan animals (Fig. 2a). The split of the $Na_V1/Na_V2(Ca_V4)$ clade from the Ca_V1–3 molecular clades occurred before the divergence of animals and
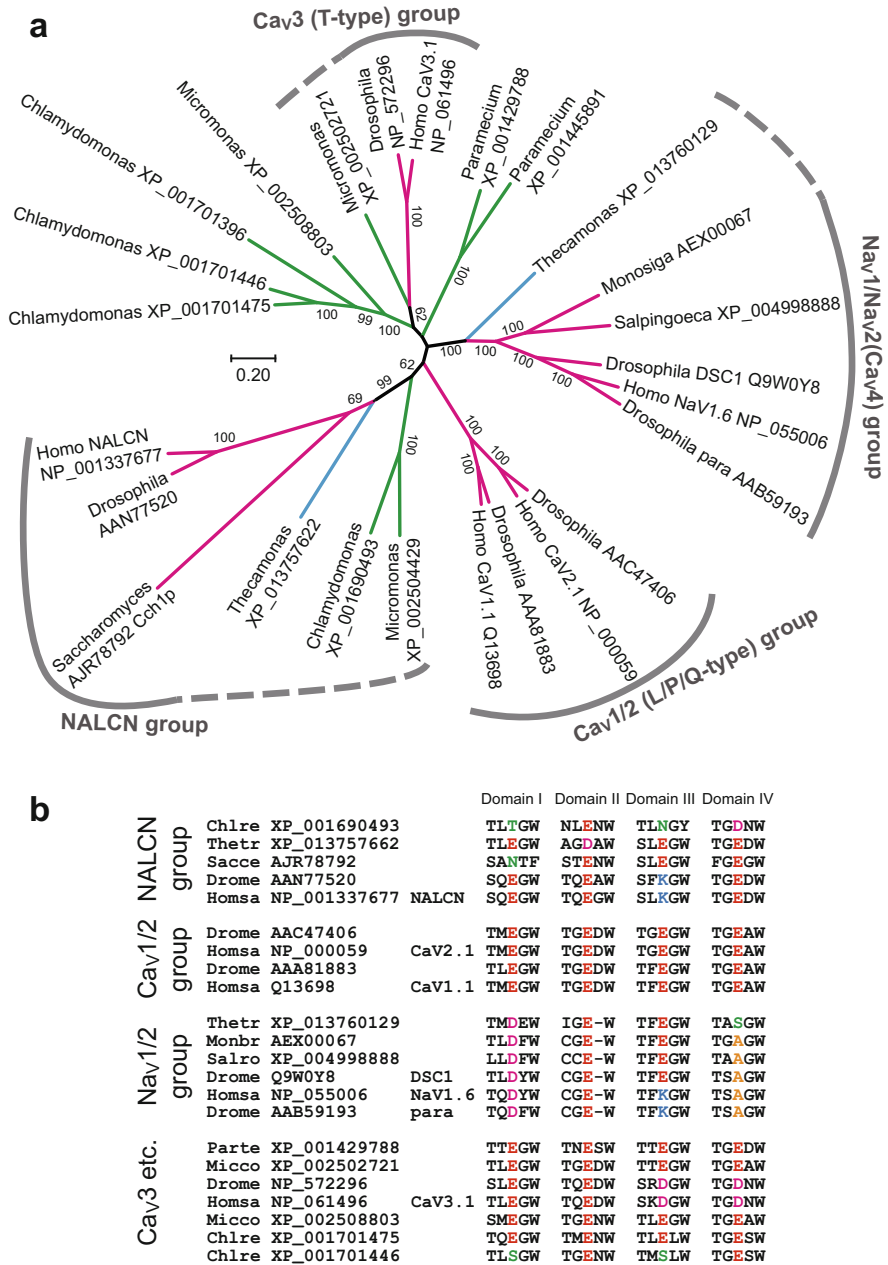
Fig. 2 Molecular phylogeny of eukaryotic 24-TM channels. (**a**) An unrooted maximum-likelihood tree of 24-TM channels found in green algae (*Chlamydomonas reinhardtii*, *Micromonas commoda*), the ciliate (*Paramecium tetraurelia*), the fungi (*Saccharomyces cerevisiae*), the apusozoan flagellate (*Thecamonas trahens*), choanoflagellates (*Monosiga brevicollis*, *Salpingoeca rosetta*), and metazoans (*Drosophila melanogaster*, *Homo sapiens*). Accession numbers of the

choanoflagellates, the protozoan group most closely related to the metazoan clade (Zakon 2012; Liebeskind et al. 2012; Moran et al. 2015). NALCN-like sequences are also found in fungi, and the history of this family can be traced back to the origin of opisthokonta, the monophyletic group containing animals, choanoflagellates, and fungi (Torruella et al. 2011; Liebeskind et al. 2012). Figure 2a shows here that in fact the representative unicellular eukaryotes distantly related with each other, such as the yeast *Saccharomyces*, the ciliate *Paramecium*, and green algae *Chlamydomonas* and *Micromonas*, possess different types of the 24-TM channel proteins. For instance, *Saccharomyces*, *Chlamydomonas*, and *Micromonas* express a 24-TM channel related to NALCN of animals, while *Paramecium*, *Chlamydomonas*, and *Micromonas* use other types of 24-TM channels closer to Na_Vs or Ca_Vs of animals (Fig. 2a). This suggests that the gene duplication of NALCN, Na_V, and Ca_V (even between $Ca_V1/2$ and Ca_V3 families) preceded the split of Unikonta (including animals, fungi, and amoebozoans) and Bikonta (plants, algae, etc.), namely, had occurred close to or before the origin of eukaryotes (Fig. 2a) (see also the phylogenetic views of eukaryotic lineages in Roger and Simpson 2008; Rogozin et al. 2009; Cavalier-Smith 2010). Despite the deep origin of the voltage-gated 24-TM Ca^{2+}/Na^+ channels, it is also known that many eukaryotic groups lack the genes of them, probably because of secondary loss. Brunet and Arendt (2015) argued that the losses of 24-TM Na_V/Ca_V channels that had happened in varied eukaryote lineages are tightly correlated with the absence of flagella in those organisms. The Ca_V channels of *Paramecium* and *Chlamydomonas* are localized in the membrane of their cilia/flagella, in which the channels function to generate APs to change flagellar/ciliary beating waveforms (Machemer and Ogura 1979; Fujiu et al. 2009). The flagellar localization of the 24-TM Ca_V/Na_V channels may be a preadaptation for the later emergence of neurons (Brunet and Arendt 2015).

While the phylogenetic relationships among the protein sequences from various eukaryotes are based on overall sequence similarities, the ion-selectivity filter signatures (D/E/K/A, E/E/E/E, E/E/D/D, and E/E/K/E in mammalian Na_V1, $Ca_V1/2$, Ca_V3, and NALCN, respectively) were established relatively recently (Fig. 2b) (Liebeskind et al. 2011, 2012). This means that the specific ion selectivity of each family may have changed over the course of evolution. For instance, the D/E/K/A pore signature of Na_V1 is thought to have emerged at the origin of

Fig. 2 (continued) sequences are indicated in the tree. The groups of $Na_V1/Na_V2(Ca_V4)$, $Ca_V1/2$, Ca_V3, and NALCN and their extended clades are indicated with *gray* solid and *dashed lines*. The bootstrap values over 60 are shown. The tree was constructed using the WAG model on MEGA7 from gap-free 847 amino acid positions aligned by MUSCLE program. (**b**) The pore signatures (at the putative ion-selectivity filter in the P-loops) of the eukaryotic 24-TM channels. The signature sequences were obtained from the alignment used for constructing the tree shown in (**a**). The species codes (first column) made of the first three and two letters from the genus and species name, respectively, and accession numbers (second column) are shown. The amino acids at the pore signatures are highlighted with colors [Asp (D), *magenta*; Glu (E), *red*; Lys (K), *blue*; Ala (A), *yellow*; other polar amino acids, *green*]

Bilateria (the clade of animals with bilateral body plans). The evidence is that all Na_V-type 24-TM genes found so far in choanoflagellates (the closest relatives to metazoans) (*Monosiga* and *Salpingoeca* in Fig. 2) and in ctenophores and placozoans (non-bilaterian metazoans), encode the D/E/E/A filter motif, not D/E/K/A, which implies the $Na_V2(Ca_V4)$-type pore signature is original (Liebeskind et al. 2011; Zakon 2012; Gur Barzilai et al. 2012; Moran et al. 2015). Cnidarians, another major non-bilaterian metazoan group, express several isoforms of Na_V-like 24-TM polypeptides with D/E/E/A (called $Na_V2.1$, 2.3, and 2.4), D/E/E/T ($Na_V2.2$), and D/K/E/A ($Na_V2.5$) pore signatures, and a phylogenetic analysis suggested that the latter two of the isoforms were derived from the first (Fig. 3) (Gur Barzilai et al. 2012; Moran et al. 2015). The cnidarian D/K/E/A channels ($Na_V2.5$) are presumably Na^+-selective, representing convergent evolution of Na^+-selective channels that was independent from the origin of the D/E/K/A Na_V1 subfamily in bilaterians (see below) (Anderson et al. 1993; Gur Barzilai et al. 2012). This molecular parallel evolution may be related to independent acquisitions of large bodies moving fast in cnidarians (e.g., jellyfish) and in bilaterians. On the other hand, the pore signature of cnidarian NALCN-like genes is commonly E/E/E/E, which likely ensures Ca^{2+} selectivity, while those in all known bilaterians have E/E/K/E at the selectivity filter, making the channels to be cation nonselective (Lu et al. 2007; Liebeskind et al. 2012).

From the evidence summarized above, it can be predicted that at their origin animals possessed two or three Ca_V subfamily genes, one $Na_V2(Ca_V4)/Na_V1$ sub-family gene and one NALCN-like gene (Moran and Zakon 2014; Moran et al. 2015). Interestingly, none of the channels are Na^+-selective, but are Ca^{2+}-preferential. Animals may have evolved as organisms lacking voltage-gated Na^+-selective channels, and the true metazoan Na^+ channels, Na_V1s with the D/E/K/A signature, emerged in a bilaterian ancestor via gene duplication and diversification that at the same time gave rise to the $Na_V2(Ca_V4)$ subfamily.

4 Evolution of Bilaterians and Voltage-Gated Sodium Channel Proteins

Bilateria is composed of animals having bilateral body plans, which are classified into three superphyla, Deuterostomia, Lophotrochozoa, and Ecdysozoa. These animal groups share a basic repertoire of 24-TM ion channel paralogues of three subtypes of Ca_V (Ca_V1–3), two of $Na_V1/Na_V2(Ca_V4)$, and one of NALCN leak channel. The molecular phylogenetic analysis suggests that the Na_V1 subfamily was diverged from the $Na_V2(Ca_V4)$ subfamily and originated in the last common ancestor of bilaterians (Fig. 3) (Liebeskind et al. 2011; Moran et al. 2015). The origin of Na_V1 in fact correlated with the development of the D/E/K/A pore signature and therefore represents the occurrence of "true" Na^+ selectivity in 24-TM channels (Fig. 3) (Liebeskind et al. 2011). This channel enabled bilateral animals to specifically utilize Na^+, the most abundant cation within the environment in which they had adapted. Combined with the function of the Na^+ pump (Na,K-ATPase), Na_V1 would have conferred a fast electric responsiveness to excitable cells by means of the large
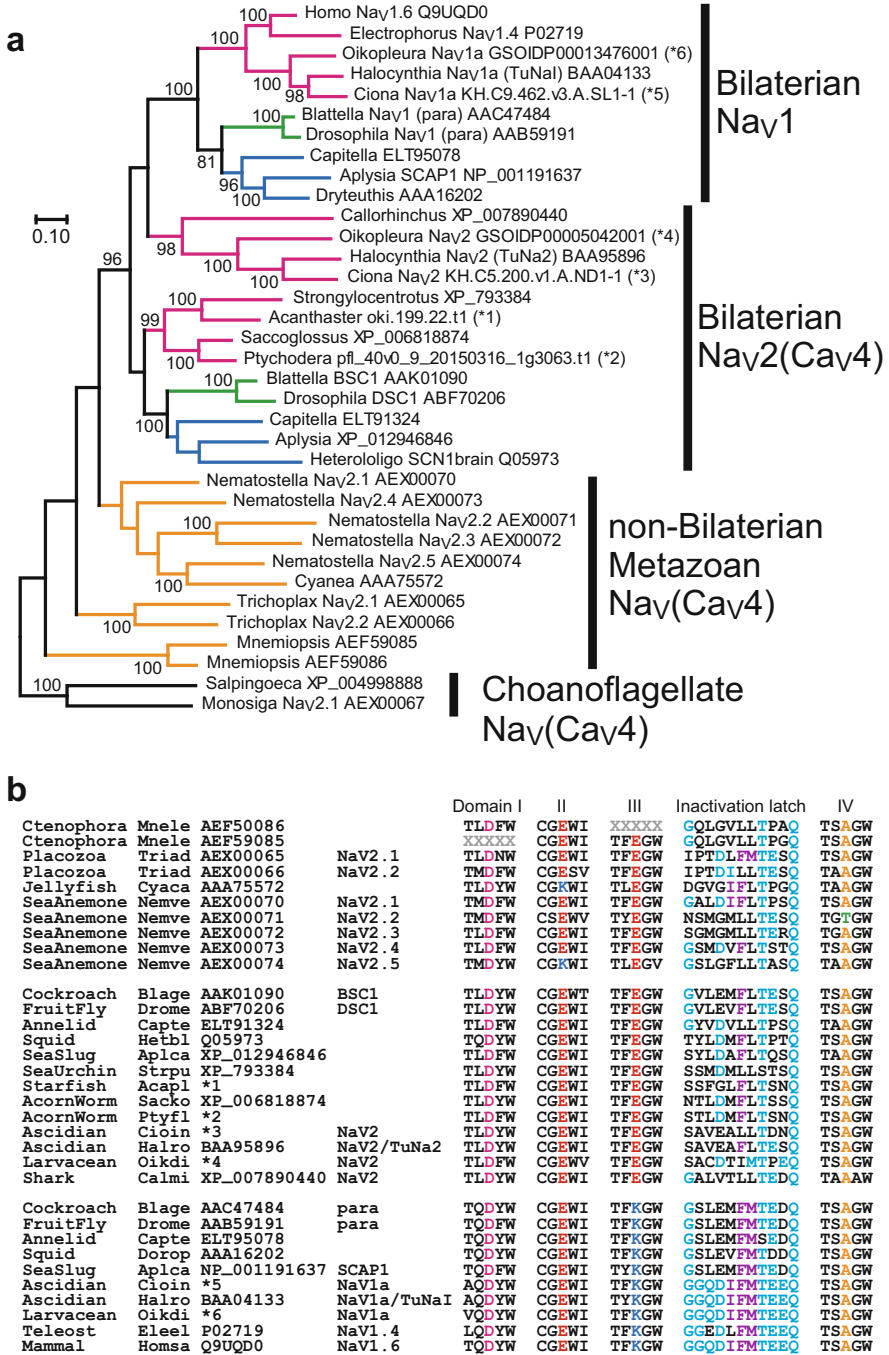
Fig. 3 Molecular phylogeny of metazoan Na$_V$1/Na$_V$2(Ca$_V$4) channels. (**a**) A maximum-likelihood tree of Na$_V$-related channels from the ctenophore (*Mnemiopsis leidyi*), the placozoan (*Trichoplax adhaerens*), the jellyfish (*Cyanea capillata*), the sea anemone (*Nematostella vectensis*), squids

driving force across the membrane. Na_V1 would also be important in that it could mediate steep depolarization without direct stimulation of the intracellular processes triggered by Ca^{2+}, a major second messenger in the wide variety of unicellular and multicellular organisms. It is also possible the inactivation latch in the loop between domains III and IV developed at the same time (Fig. 3b), which would have facilitated fast recovery to the resting state of membrane potential and thus enabled cells to minimize the changes in intracellular ionic conditions. Importantly, the molecular development of Na_V1 would be related not only to fast generation/propagation of APs but also to the occurrence of refractory periods after depolarization. Repetitive excitation of neurons is facilitated by these characteristics of Na_V1, which enables the nerves to encode neural signals based on the AP frequencies. Fast neural transmission would have supported evolution of larger bodies, and the ability to inactivate itself can ensure unidirectional flow of signals within the neural network. This would have offered segregation of input (sensory) systems from output (motor) systems, permitting development of the CNS.

The evolutionary emergence and divergence of bilaterians represents the geographical event called the "Cambrian explosion." It is inspiring to consider that the origin of Na_V1 is concordant with the evolution of bilaterians. Paleontologists have suggested that predator-prey relationships were established during the Cambrian era, which stimulated increases in body size and complexity and also the sophistication of sensory organs, leading to acceleration of movement and further elaboration of the CNS (Conway-Morris 1986; Gould 1990; Parker 2003). One hypothesis has proposed that development of eyes was a key step in this so-called evolutionary big bang (Parker 2003). Given this context, it would be reasonable to predict that

Fig. 3 (continued) (*Doryteuthis opalescens*, *Heterololigo bleekeri*), the sea slug (*Aplysia californica*), the annelid worm (*Capitella teleta*), the fruit fly (*Drosophila melanogaster*), the cockroach (*Blattella germanica*), acorn worms (*Ptychodera flava*, *Saccoglossus kowalevskii*), the starfish (*Acanthaster planci*), the sea urchin (*Strongylocentrotus purpuratus*), ascidians (*Ciona intestinalis*, *Halocynthia roretzi*), the larvacean (*Oikopleura dioica*), the elephant fish chimaera (*Callorhinchus milii*), the electric eel (*Electrophorus electricus*), and humans (*Homo sapiens*). Monophyly of bilaterian Na_V1s is evident, while that of $Na_V2(Ca_V4)$ channels is not clear here. The sequences from non-bilaterian metazoans, ecdysozoans, lophotrochozoans, and deuterostomes are labeled with *yellow*, *blue*, *green*, and *magenta* branches, respectively. NCBI accession numbers and other ID codes are indicated in the tree. The sequences of *O. dioica* are obtained from OikoBase (http://oikoarrays.biology.uiowa.edu/Oiko/); those of *C. intestinalis* are from Ghost database (http://ghost.zool.kyoto-u.ac.jp/cgi-bin/gb2/gbrowse/kh/); those of *A. planci* and *P. flava* are from the OIST genome browsers (http://marinegenomics.oist.jp/gallery/gallery/index). The bootstrap values over 80 are shown. The tree was constructed using the WAG model on MEGA7 from gap-free 812 amino acid positions aligned by MUSCLE program. (**b**) The pore signatures and the region corresponding to the inactivation latch in metazoan Na_V-related channels. The sequences shown are mostly identical to those in (**a**). The species codes and color codes are same as in Fig. 2. Sequences corresponding to core triplet of the inactivation latch (I-F-M) are also marked by *purple*. *Cyan* residues indicate the amino acids identical to those around the inactivation latch of the mammalian $Na_V1.6$. *1-*6: the genemodel IDs are shown in (**a**) to identify the sequences in the genome browser of each organism

the molecular phylogenetic origin of Na_V1 provided a physiological basis for the bilaterian ancestor that potentiated the explosive evolution.

Na_V1 originated through gene duplication and diversification that gave rise to the $Na_V2(Ca_V4)$ as well (Fig. 3a). Consequently, most bilaterians express two subtypes of Na_V family components, Na_V1 and $Na_V2(Ca_V4)$. For example, the genome of *Drosophila melanogaster* harbors *para*, which encodes a Na_V1-type channel, and *DSC1*, which encodes a $Na_V2(Ca_V4)$ channel (Salkoff et al. 1987; Ramaswami and Tanouye 1989; Loughney et al. 1989; Hong and Ganetzky 1994; Kulkarni et al. 2002; Zhang et al. 2013). Major invertebrate lineages, such as mollusks, annelids, arthropods, and chordates all express $Na_V2(Ca_V4)$ proteins in addition to Na_V1. $Na_V2(Ca_V4)$ family proteins contain voltage sensors – i.e., S4 segments containing evenly spaced, positively charged residues, and their pore signature is generally D/E/E/A. When exogenously expressed in *Xenopus* oocytes, $Na_V2(Ca_V4)$ family proteins from the cockroach and honeybee (called BSC1 and $AmCa_V4$, respectively) are more permeable to the divalent cations Ca^{2+} and Ba^{2+} than to Na^+ (Zhou et al. 2004; Gosselin-Badaroudine et al. 2016). These channels are reportedly insensitive to TTX, exhibit relatively slow activation and inactivation, and can be blocked by Cd^{2+} or Zn^{2+}. Phenotypic analyses of *DSC1* gene mutants in *Drosophila* have suggested its functions in olfaction or odor-responsive behavior and also in stabilizing the performance of neural circuits under stresses (Kulkarni et al. 2002; Zhang et al. 2013).

While bilateral animals share orthologues of Na_V1 and $Na_V2(Ca_V4)$, it has also been revealed that some animal lineages have lost either the Na_V1 or $Na_V2(Ca_V4)$ subtype, or both. It is well known, for example, that the genome of *Caenorhabditis elegans* contains neither Na_V1 nor $Na_V2(Ca_V4)$ (e.g., Okamura et al. 2005). Whether these paralogues are present or absent is thought to reflect the physical characteristics and lifestyle of each animal group, including body size, locomotion speed, and/or complexity of neural processing. Although the nematode lacks any Na_V-class channels, it is not true that this species is "primitive." The nematode lost this protein because it was not essential for its interstitial life. In fact, nematodes have flourished around the globe without it.

The Na_V1 family channels are absent from echinoderms and hemichordates, the group collectively called Ambulacraria, which constitutes the sister clade of the phylum Chordata (Fig. 3) (see also Widmark et al. 2011; Gur Barzilai et al. 2012). This indicates that echinoderms and hemichordates (ambulacrarians) secondarily lost the fast Na_V1, while the $Na_V2(Ca_V4)$ with the D/E/E/A pore signature typical for that subfamily remains. This suggests these animal groups are incapable of fast sodium spikes. These animals are small during the larval stage (about 0.1–5.0 mm), and the adults (about 1–10 cm or more sometimes) are generally slow moving. They are not fast predators but protective; echinoderm adults are covered with calcite skeletons, and sometimes also with spines, while hemichordates are generally buried in the seafloor. They develop an ectodermal nerve net over the entire body, and their CNS is relatively rudimentary (Hyman 1955; Holland 2003, 2016; Nomaksteinsky et al. 2009). Their evolutionary status may be regarded like an atavism – i.e., reminiscent of the status of animals before the origin of bilaterians. In other words,

they live a "slow life" that is a consequence of the loss of Na_V1. On the contrary, the last common ancestor of bilaterians had a Na_V1-type channel and lived a "quick life." Therefore, the long-standing controversy around how the less centralized nervous system seen in echinoderms or hemichordates was integrated into the well-centralized nervous system of vertebrates may not be valid (for reviews, e.g., Holland 2003, 2016). It is noteworthy that recent analyses of the CNS of a polychaete annelid (ragworm) provided surprising evidence of its deep anatomical similarity to the vertebrate CNS (Tessmar-Raible et al. 2007; Tomer et al. 2010; Vergara et al. 2017). A well-centralized nervous system in the last common ancestor of bilaterians would be consistent with the evolution of Na_V1.

5   Voltage-Gated Sodium Channels in Chordates

As the bilaterians diversified, the chordate lineage led to vertebrates and two other animal groups, the amphioxi (cephalochordates, lancelets) and tunicates (urochordates). Recent comparative genomic analyses showed that the amphioxi diverged first within these three groups, and tunicates and vertebrates form a sister group (Delsuc et al. 2006; Putnam et al. 2008). Amphioxi and tunicates provided "observation windows" for researchers to investigate past situations before establishment of vertebrate bodies.

Amphioxi inhabit sandy shores and live as filter feeders. They are able to swim out of the sand and dive back into it very quickly. While they develop segmented somites, they lack developed eyes or an expanded brain (Willey 1894). Their repertoire of Na_V-related α subunits also appears primitive. An amphioxus likely possesses five genes encoding $Na_V1/Na_V2(Ca_V4)$ channel α subunits. At least three of the genes are classified as Na_V1 family, and the other two are in the $Na_V2(Ca_V4)$ clade (Fig. 4a). The three Na_V1 channels of amphioxi are paralogous with each other and share the D/E/K/A pore signature. On the other hand, the differences in their amino acid sequences are considerable, implying differing functions of the isoforms and situation-dependent differential utilizations (tissue- or life stage-specific expression, etc.). A clearer sign of functional specificity is seen in the $Na_V2(Ca_V4)$ proteins; the one (depicted as Na_V2a in Fig. 4) contains a D/D/Q/A, not the D/E/E/A, pore signature at the ion-selectivity filter. Although we do not know the ion permeability of amphioxus Na_V2a, it is conceivable the D/D/Q/A signature invests the excitable membranes of this animal with a regulatory option. Examination of these organisms enables us to monitor an "evolutionary experiment" carried out through gene duplication before the emergence of vertebrates (Ohno 1970).

Similar traces are also found in the tunicate lineage, which possess four types of $Na_V1/Na_V2(Ca_V4)$ proteins. Ascidians, constituting a representative tunicate class, abundantly distribute along the shores around the world. Their adult form is sessile, while the larvae are in the form of tiny tadpoles that swim in the sea. Ascidians have been utilized as a research model, because of their kinship to vertebrates, but also because of their abundance and the availability of mature gametes among other
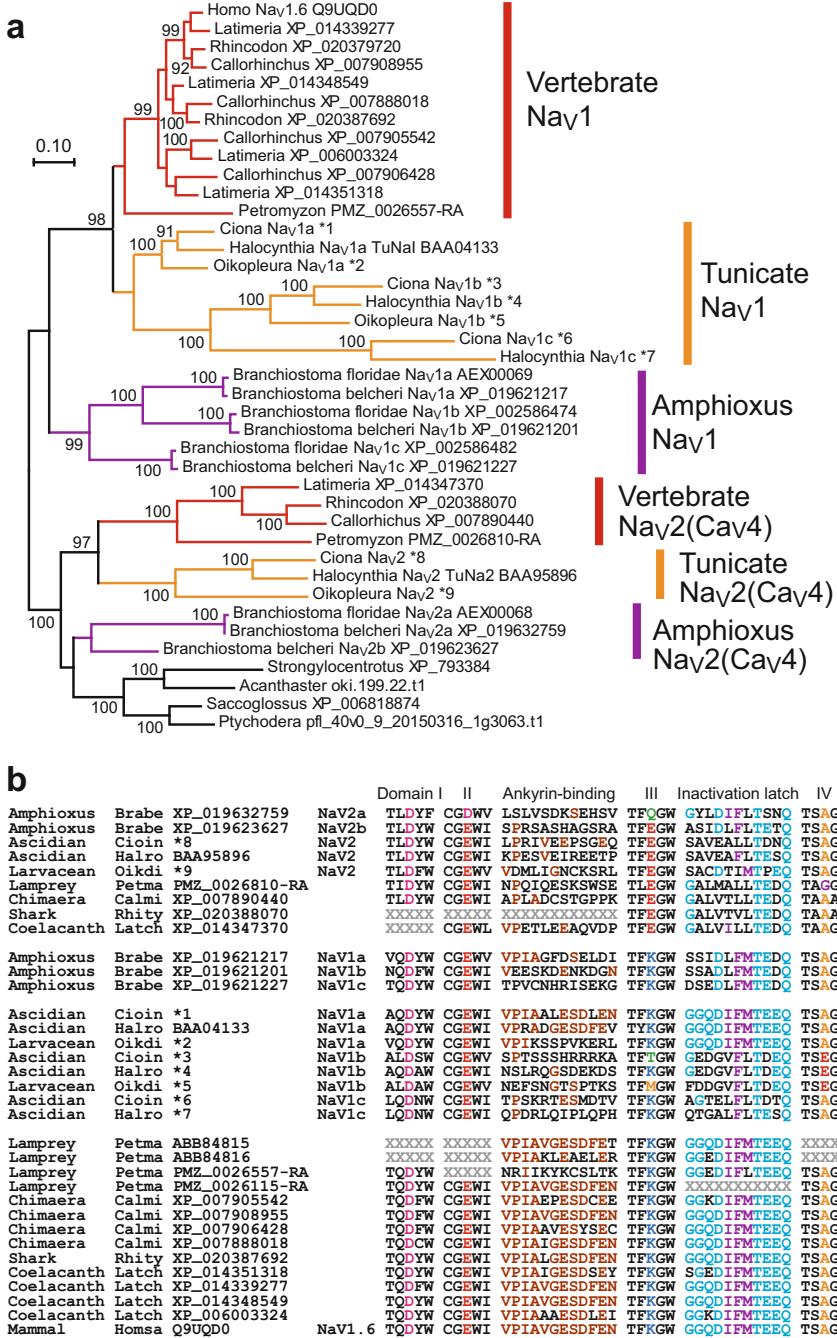
a

Scale: 0.10

Vertebrate Nav1:
- Homo Nav1.6 Q9UQD0
- Latimeria XP_014339277 — 99
- Rhincodon XP_020379720
- Callorhinchus XP_007908955 — 92
- Latimeria XP_014348549 — 99
- Callorhinchus XP_007888018
- Rhincodon XP_020387692 — 100
- Callorhinchus XP_007905542 — 100
- Latimeria XP_006003324
- Callorhinchus XP_007906428
- Latimeria XP_014351318
- Petromyzon PMZ_0026557-RA

(98)

Tunicate Nav1:
- Ciona Nav1a *1 — 91
- Halocynthia Nav1a TuNaI BAA04133 — 100
- Oikopleura Nav1a *2
- Ciona Nav1b *3 — 100
- Halocynthia Nav1b *4 — 100
- Oikopleura Nav1b *5
- Ciona Nav1c *6 — 100
- Halocynthia Nav1c *7 — 100

Amphioxus Nav1:
- Branchiostoma floridae Nav1a AEX00069 — 100
- Branchiostoma belcheri Nav1a XP_019621217 — 100
- Branchiostoma floridae Nav1b XP_002586474 — 100
- Branchiostoma belcheri Nav1b XP_019621201
- Branchiostoma floridae Nav1c XP_002586482 — 100
- Branchiostoma belcheri Nav1c XP_019621227

(99)

Vertebrate Nav2(Cav4):
- Latimeria XP_014347370 — 100
- Rhincodon XP_020388070 — 100
- Callorhinchus XP_007890440 — 100
- Petromyzon PMZ_0026810-RA

(97)

Tunicate Nav2(Cav4):
- Ciona Nav2 *8 — 100
- Halocynthia Nav2 TuNa2 BAA95896 — 100
- Oikopleura Nav2 *9

Amphioxus Nav2(Cav4):
- Branchiostoma floridae Nav2a AEX00068 — 100
- Branchiostoma belcheri Nav2a XP_019632759
- Branchiostoma belcheri Nav2b XP_019623627

(100)
- Strongylocentrotus XP_793384 — 100
- Acanthaster oki.199.22.t1
- Saccoglossus XP_006818874 — 100
- Ptychodera pfl_40v0_9_20150316_1g3063.t1 — 100

b

				Domain I	II	Ankyrin-binding	III	Inactivation latch	IV
Amphioxus	Brabe	XP_019632759	NaV2a	TLDYF	CGDWV	LSLVSDKSEHSV	TFQGW	GYLDIFLTSNQ	TSAGW
Amphioxus	Brabe	XP_019623627	NaV2b	TLDYW	CGEWI	SPRSASHAGSRA	TFEGW	ASIDLFLTETQ	TSAGW
Ascidian	Cioin	*8	NaV2	TLDYW	CGEWI	LPRIVEEPSGEQ	TFEGW	SAVEALLTDNQ	TSAGW
Ascidian	Halro	BAA95896	NaV2	TLDYW	CGEWI	KPESVEIREETP	TFEGW	SAVEAFLTESQ	TSAGW
Larvacean	Oikdi	*9	NaV2	TLDFW	CGEWV	VDMLIGNCKSRL	TFEGW	SACDTIMTPEQ	TSAGW
Lamprey	Petma	PMZ_0026810-RA		TIDYW	CGEWI	NPQIQESKSWSE	TLEGW	GALMALLTEDQ	TAGGW
Chimaera	Calmi	XP_007890440		TLDYW	CGEWI	APLADCSTGPPK	TFEGW	GALVTLLTEDQ	TAAAW
Shark	Rhity	XP_020388070		XXXXX	XXXXX	XXXXXXXXXXXX	TFEGW	GALVTVLTEDQ	TAAAW
Coelacanth	Latch	XP_014347370		XXXXX	CGEWL	VPETLEEAQVDP	TFEGW	GALVILLTEDQ	TAAGW
Amphioxus	Brabe	XP_019621217	NaV1a	VQDFW	CGEWV	VPIAGFDSELDI	TFKGW	SSIDLFMTEDQ	TSAGW
Amphioxus	Brabe	XP_019621201	NaV1b	NQDFW	CGEWI	VEESKDENKDGN	TFKGW	SSADLFMTEDQ	TSAGW
Amphioxus	Brabe	XP_019621227	NaV1c	TQDYW	CGEWI	TPVCNHRISEKG	TFKGW	DSEDLFMTEDQ	TSAGW
Ascidian	Cioin	*1	NaV1a	AQDYW	CGEWI	VPIAALESDLEN	TFKGW	GGQDIFMTEEQ	TSAGW
Ascidian	Halro	BAA04133	NaV1a	AQDYW	CGEWI	VPRADGESDFEV	TYKGW	GGQDIFMTEEQ	TSAGW
Larvacean	Oikdi	*2	NaV1a	VQDYW	CGEWI	VPIKSSPVKERL	TFKGW	GGQDIFMTEEQ	TSAGW
Ascidian	Cioin	*3	NaV1b	ALDSW	CGEWV	SPTSSSHRRRKA	TFTGW	GEDGVFLTDEQ	TSEGW
Ascidian	Halro	*4	NaV1b	AQDAW	CGEWI	NSLRQGSDEKDS	TFKGW	GEDGVFLTDEQ	TSEGW
Larvacean	Oikdi	*5	NaV1b	ALDAW	CGEWV	NEFSNGTSPTKS	TMGW	FDDGVFLTDEQ	TSEGW
Ascidian	Cioin	*6	NaV1c	LQDNW	CGEWI	TPSKRTESMDTV	TFKGW	AGTELFLTDTQ	TSAGW
Ascidian	Halro	*7	NaV1c	LQDNW	CGEWI	QPDRLQIPLQPH	TFKGW	QTGALFLTESQ	TSAGW
Lamprey	Petma	ABB84815		XXXXX	XXXXX	VPIAVGESDFET	TFKGW	GGQDIFMTEEQ	XXXXX
Lamprey	Petma	ABB84816		XXXXX	XXXXX	VPIAKLEAELER	TFKGW	GGEDIFMTEEQ	XXXXX
Lamprey	Petma	PMZ_0026557-RA		TQDYW	XXXXX	NRIIKYKCSLTK	TFKGW	GGEDIFLTEEQ	TSAGW
Lamprey	Petma	PMZ_0026115-RA		TQDYW	CGEWI	VPIAVGESDFEN	TFKGW	XXXXXXXXXXX	TSAGW
Chimaera	Calmi	XP_007905542		TQDFW	CGEWI	VPIAEPESDCEE	TFKGW	GGKDIFMTEEQ	TSAGW
Chimaera	Calmi	XP_007908955		TQDFW	CGEWI	VPIAVGESDFEN	TFKGW	GGQDIFMTEEQ	TSAGW
Chimaera	Calmi	XP_007906428		TQDFW	CGEWI	VPIAAVESYSEC	TFKGW	GGQDIFMTEEQ	TSAGW
Chimaera	Calmi	XP_007888018		TQDCW	CGEWI	VPIAIGESDFEN	TFKGW	GGQDIFMTEEQ	TSAGW
Shark	Rhity	XP_020387692		TQDYW	CGEWI	VPIALGESDFEN	TFKGW	GGQDIFMTEEQ	TSAGW
Coelacanth	Latch	XP_014351318		TQDYW	CGEWI	VPIAIGESDSEY	TFKGW	SGEDIFMTEEQ	TSAGW
Coelacanth	Latch	XP_014339277		TQDFW	CGEWI	VPIAVGESDFEN	TFKGW	GGQDIFMTEEQ	TSAGW
Coelacanth	Latch	XP_014348549		TQDYW	CGEWI	VPIAVGESDFEN	TFKGW	GGQDIFMTEEQ	TSAGW
Coelacanth	Latch	XP_006003324		TQDYW	CGEWI	VPIAAAESDLEI	TFKGW	GGKDIFMTEEQ	TSAGW
Mammal	Homsa	Q9UQD0	NaV1.6	TQDYW	CGEWI	VPIAVGESDFEN	TFKGW	GGQDIFMTEEQ	TSAGW

Fig. 4 Molecular phylogeny of chordate Nav1 and Nav2(Cav4) channels. (**a**) A maximum-likelihood tree of Nav-related channels from acorn worms (*Ptychodera flava*, *Saccoglossus kowalevskii*), the starfish (*Acanthaster planci*), the sea urchin (*Strongylocentrotus purpuratus*), amphioxi (*Branchiostoma belcheri* and *B. floridae*), ascidians (*Ciona intestinalis*, *Halocynthia*

features. Ascidians have contributed to ion channel studies through the "mosaicism" of their embryogenesis. Historical studies revealed that neuron-like Na^+ spikes could be evoked in the neural cell-lineage blastomere of embryos whose cleavage was arrested using an inhibitor of cytokinesis (Takahashi and Yoshii 1981; Takahashi and Okamura 1998). Developmental expression of this Na^+ current in the neural cell-lineage blastomere is dependent on a fibroblast growth factor-like inductive signal from a neighboring endomesodermal blastomere, which represents neural induction. This process of differentiation in membrane excitability is firmly correlated with the gene expression of a Na_V1 channel, originally called TuNaI (referred to as Na_V1a here) (Okado and Takahashi 1988; Okamura et al. 1994; Takahashi and Okamura 1998). This Na_V1a α subunit is actually expressed in all known neuronal types (Okamura et al. 1994; Okada et al. 1997). Later studies carried out before and after the genomic sequencing of several species of ascidians revealed that ascidians have four genes encoding Na^+ channel α subunits (Nagahora et al. 2000; Okamura et al. 2005; Brozovic et al. 2016). One encodes Na_V1a (TuNaI) containing the typical D/E/ K/A pore signature, an inactivation latch with the I-F-M triplet between domains III and IV, and a sequence similar to the ankyrin-binding motif found in the loop between domains II and III of vertebrate Na_V1s (see below). Another encodes a $Na_V2(Ca_V4)$ subfamily protein containing the typical D/E/E/A pore signature (Na_V2, previously called TuNa2), but lacking clear consensus sequences for the inactivation latch and ankyrin-binding motif (Fig. 4) (Nagahora et al. 2000). This gene encoding $Na_V2(Ca_V4)$ is also expressed in some, but not all, neurons in ascidians (Nagahora et al. 2000). The nested patterns of Na_V1 and $Na_V2(Ca_V4)$ gene expression are reminiscent of the patterns of *para* and *DSC1* expression in *Drosophila* embryos (Hong and Ganetzky 1994).

Fig. 4 (continued) roretzi), the larvacean (*Oikopleura dioica*), the lamprey (*Petromyzon marinus*), the elephant fish chimaera (*Callorhinchus milii*), the whale shark (*Rhincodon typus*), the coelacanth (*Latimeria chalumnae*), and humans (*Homo sapiens*). The clades of Na_V1 and $Na_V2(Ca_V4)$ are clearly divided. Vertebrates possess $Na_V2(Ca_V4)$. The sequences from amphioxi, tunicates (ascidians and larvaceans), and vertebrates are labeled with *purple*, *yellow*, and *red* branches, respectively. NCBI accession numbers and other ID codes are mostly indicated in the tree. *1-*9 indicate the genemodel IDs in the genome browser of each organism: *1, KH.C9.462.v3.A.SL1–1; *2, GSOIDP00013476001; *3, KH.C1.1161.v1.A.ND1–1; *4, Harore.CG.MTP2014.S1.g14830; *5, GSOIDP00011229001; *6, KH.C10.502.v2.A.SL1–1; *7, Harore.CG.MTP2014.S25.g02359; *8, KH.C5.200.v1.A.ND1–1; *9, GSOIDP00005042001. The *O. dioica* sequences are obtained from OikoBase (http://oikoarrays.biology.uiowa.edu/Oiko/); the *C. intestinalis* sequences are from Ghost database (http://ghost.zool.kyoto-u.ac.jp/cgi-bin/gb2/gbrowse/kh/); the *H. roretzi* sequences are from Aniseed database (https://www.aniseed.cnrs.fr/); the *P. marinus* sequences are from the UCSC genome browser gateway (http://genome-asia.ucsc.edu/cgi-bin/hgGateway); and the *A. planci* and *P. flava* sequences are from the OIST genome browsers (http://marinegenomics.oist. jp/gallery/gallery/index). The bootstrap values over 90 are shown. The tree was constructed using the WAG model on MEGA7 from gap-free 526 amino acid positions aligned by MUSCLE program. (**b**) The pore signatures and the regions corresponding to ankyrin-binding motif and the inactivation latch in chordate Na_V-related channels. The species codes and color codes are as used in Figs. 2 and 3. Amino acids identical to the mammalian $Na_V1.6$ ankyrin-binding motif are indicated by *brown*. *1-*9: the genemodel IDs identical to those in (**a**)

The other two channels in ascidians, called here Na_V1b and Na_V1c (previously named Na_V3 and 4, respectively, in Okamura et al. 2005), are categorized in the Na_V1 family, and the tunicate Na_V1a, b, and c constitute a clade different from that including the vertebrate Na_V1s (Fig. 4a). While the ion-selectivity filter signature of the tunicate Na_V1c is the same as that in typical Na_V1-type channels (D/E/K/A), Na_V1b exhibits a D/E/(K or T or M)/E pore signature (Fig. 4b) (see also Widmark et al. 2011). We do not know the ion permeability of either channel. Temporal expression patterns estimated from the counts of expressed sequenced tags (ESTs) in the ascidian *Ciona intestinalis* (Satou et al. 2003) suggests the tunicate Na_V1a (TuNaI) is expressed in the larval and adult nervous systems which is consistent with in situ analyses of this gene expression pattern (Okamura et al. 1994, 2005; Okada et al. 1997). Na_V2 is estimated to be expressed in the nervous systems of larvae and juveniles, and possibly on the juvenile endostyle, which is an organ putatively homologous to the vertebrates' thyroid gland. The EST counts suggest expression of Na_V1b occurs during the larval stage. Our preliminary examination of the spatial expression pattern in *C. intestinalis* showed that the Na_V1b gene is expressed in neurons in the CNS and PNS and in some of the muscle cells in the larva. The EST counts predict a small amount of Na_V1c is expressed during the larval stage, though our preliminary in situ hybridization analysis did not detect any clear signal during the larval stage. Also, intriguing is the detection of EST counts for Na_V1b and Na_V1c in mature hermaphroditic adults producing gametes, not in young immature adults. In the eggs of ascidians, steep membrane depolarization is evoked in response to fertilization, which is known to be mediated by an unknown voltage-gated Na^+ channel that is somewhat permeable to Ca^{2+} along with Na^+ (Okamoto et al. 1977; Fukushima 1981; Okamura and Shidara 1987). Thus Na_V1b and/or Na_V1c may be involved in this process.

Single-channel recordings from cleavage-arrested neuronal blastomeres of the ascidian *Halocynthia roretzi* support this view. The electrophysiology has uncovered three types of voltage-gated sodium currents that turn over with time after fertilization to matured stage (Okamura and Shidara 1990a, b). The "Type A" Na^+ current shows only one decay phase during voltage-dependent inactivation, suggesting that a single type of Na_V is responsible for this current. Type A currents are seen in every blastomere within early embryos, and its expression level appears highest at the gastrula stage. This type of Na^+ current is identical to that in the fertilization potential of *Halocynthia* eggs represented by a Na^+-dependent AP (Fukushima 1981). The Na_V current in *Halocynthia* eggs is insensitive to TTX but is highly sensitive to scorpion toxin and local anesthetics (Okamoto et al. 1977). These data suggest that the tunicate Na_V1b, which has an atypical pore signature and is thus resistant to TTX, is involved in the Type A current. On the other hand, voltage-dependent inactivation of the "Type C" current shows two different, fast and slow, phases of decay (Okamura and Shidara 1987), which is reminiscent of the Nav1.6 channel in mammalian neurons. The Type C is the most predominant in differentiated neuronal blastomeres and is suppressed by microinjection of antisense DNA targeting the *Halocynthia* Na_V1a gene *TuNaI* (Okamura et al. 1994). During the short period between the disappearance of Type A and appearance of Type C currents during the

developmental course of neural-type membrane excitability, an unusual voltage-gated Na^+ current, "Type B," is transiently expressed (Okamura and Shidara 1990a). This current shows persistent gating behavior with multiple short openings (burst activity). At present, the relationship between the classically characterized diversity of voltage-gated Na^+ currents and the ascidian Na_V isoforms remains unclear, though it appears that $Na_V 1a$ (TuNa1) carries Type C current. It would be interesting to know whether the tunicate $Na_V 1b$ or $Na_V 1c$ carries the Type A current and what underlies the Type B current.

The tree topology shown in Fig. 4 suggests that the ancestor of tunicate $Na_V 1$ paralogues became the seed from which there was further molecular evolution of the $Na_V 1$ channels in modern vertebrates. The $Na_V 1a$ of tunicates shares an ankyrin-binding motif sequence with the vertebrate $Na_V 1s$ (Fig. 1) (Hill et al. 2008), which consists of a dozen amino acids residing in the loop between domains II and III (Fig. 4b), while the $Na_V 1b$ and $Na_V 1c$ proteins almost lost it. Similarly, the I-F-M inactivation latch that is conserved in the tunicate $Na_V 1a$ has been lost in the paralogues, $Na_V 1b$ and $Na_V 1c$ (Fig. 4b). Another ankyrin-binding motif similar to that in vertebrate $Na_V 1s$ is also found in vertebrate KCNQ2/3 ($K_V 7.2/7.3$) K^+ channels, and these motifs are crucial for ankyrin-G binding and for anchoring of $Na_V 1s$ and KCNQ2/3s at the axon initial segment (AIS) and nodes of Ranvier in myelinated neurons (Garrido et al. 2003; Lamaillet et al. 2003; Pan et al. 2006; Hill et al. 2008). The sequences of the motif in ascidians' $Na_V 1a$ varies somewhat, but ~70% of the amino acids are conserved (Fig. 4b). Even the $Na_V 1$ channel in amphioxi, depicted as *Branchiostoma* $Na_V 1a$ in Fig. 4, has ~40% identity, though we find no other traces in invertebrate $Na_V 1s$ (Fig. 4b) (Hill et al. 2008). Myelination and resultant saltatory conduction are regarded as a feature of jawed vertebrates (gnathostomes) (Zalc et al. 2008; Zalc 2016). Despite the absence of nodes of Ranvier in amphioxi and tunicates, the ankyrin-binding motif emerged in these animals and may have initiated interaction with ankyrins within neurons. This may be a key property that the ancestral gene of the tunicate $Na_V 1$ paralogues retained, and the reason it was selected as the seed for further evolution in the vertebrate lineage.

The situations seen in amphioxi and tunicates inform us that the isoforms occurring in these so-called "protochordate" organisms through gene duplication differentially evolved, leading to changes, even into the pore signature (as seen in $Na_V 1b$ of tunicates and $Na_V 2b$ of amphioxi). The gene duplications can confer specific regulatory options to each of duplicated isoforms as indicated so far (Ohno 1970). What occurred in these organisms is a prelude to what has occurred in the vertebrate lineage: another story of gene duplication and functional differentiation.

6 Evolution of $Na_V 1$ Channels in Vertebrates

The monophyletic vertebrate lineage has given rise to agnathans (hagfish and lampreys), cartilaginous fish (sharks, skates, and rays), ray-finned fish (bichirs, sturgeons, gars, bowfin, and teleosts), lobe-finned fish (paraphyletic group of

coelacanths and lungfish), and tetrapods (amphibians, reptiles, birds, and mammals) (e.g., Amemiya et al. 2013). During this process of radiation, these organisms inhabited and adapted to various environments in salt and freshwater and in wet and dry terrestrial areas. An ability for predation has been especially well developed in this animal lineage, and several ideas have been proposed in that regard (e.g., Gans and Northcutt 1983). Myelination and saltatory conduction along neuronal axons, as well as the developmental capacities derived from neural crest and placode cells that especially enhanced sensory systems, referred to as "new head," have enabled vertebrates to become larger and predatory (e.g., Gans and Northcutt 1983; Zalc 2016). The presence of active predators in turn stimulated greater ability to efficiently recognize the predators so as to escape (Parker 2003). Increased complexity of sensory inputs, higher ordered neural processing, and high-speed regulation of locomotion would have strongly supported the radiation of vertebrates under water and on land. Na_V1 function was definitely essential to those evolutionary steps.

The lamprey *Petromyzon marinus* shows multiple types of predicted transcripts encoding Na_V1 channel α subunits. Two Na_V1 isoforms have previously been identified (Hill et al. 2008; Zakon 2012), but four types, at least, may be there (Fig. 4b). Cartilaginous fish, including the elephant fish (chimaera) *Callorhinchus milii*, and the whale shark *Rhincodon typus* also appear to harbor four to five (or more) predicted transcripts for Na_V1 isoforms (Fig. 4; some sequences were too short and thus omitted here). Our molecular phylogenetic analysis suggests the Na_V1 isoforms in cartilaginous fish well reflect an original state (one gene in each of NaV1.4, NaV1.5/1.8/1.9, NaV1.6, and NaV1.1/1.2/1.3/1.7 groups), before the extensive duplication that occurred in amniotes and in teleosts (Figs. 4 and 5) (see below) (Widmark et al. 2011). It remains difficult, however, to know precise full-length sequence data for these transcripts, and there is not yet sufficient data available to draw firm conclusions.

Three lamprey Na_V1 α subunits for which longer sequence information was found in the database have the D/E/K/A pore signature. On the other hand, at least two of them contain the I-F-M inactivation ball in the loop between domains III and IV, while the third has an I-F-L triplet. The ankyrin-binding motif is conserved to varying degrees (50–100%) in their domain II-III loops (Fig. 4b). The variation in sequence motifs may represent differences of the molecular functions among them, which implies efficient "evolution by gene duplication" working in this gene family from the beginning of the vertebrate lineage (Ohno 1970).

The ankyrin-binding motif may reportedly work to locate and accumulate Na_V1s at the AIS in the neurons of lampreys (Hill et al. 2008). True myelin sheaths have not been found along the axons of lampreys, though molecular traces of myelination have been detected (Smith et al. 2013). On the other hand, the proximal portion of neuronal axons in lampreys is thinner than elsewhere along the axon. This narrow initial segment decreases local capacitance and conductance and supports the occurrence of steep APs. Localization of Na_V1 at high density in the AIS makes sense for efficient induction of APs (Hill et al. 2008; Kole and Stuart 2012), and full establishment of Na_V1 localization at the AIS via its ankyrin-binding motif may have facilitated the increase in body size of the vertebrate

Fig. 5 Molecular phylogeny of vertebrate Na$_V$1s. (**a**) A maximum-likelihood tree of Na$_V$1 α subunits from the elephant fish chimaera (*Callorhinchus milii*), the spotted gar (*Lepisosteus oculatus*), the teleost zebrafish (*Danio rerio*), the coelacanth (*Latimeria chalumnae*),

ancestor. This AIS machinery may be a preadaptation for the evolution of nodes of Ranvier and saltatory conduction in gnathostomes (jawed vertebrates). KCNQ2/3 (Kv7.2/7.3) channels emerged in gnathostomes and, together with Na_V1s, were directed toward the AIS and nodes of Ranvier via their ankyrin-binding motifs, concomitantly with the evolutionary appearance of true myelination (Hill et al. 2008). This innovation would not only change neuronal morphology, but would greatly accelerate the rates of signal relay and processing among sensory organs, neurons themselves, and effectors, which would in turn contribute to the evolution of jaws and the predatory lifestyle.

Interestingly, the genomes of the lamprey, cartilaginous fish, and the coelacanth *Latimeria* possess the gene for $Na_V2(Ca_V4)$ channel (Fig. 4). The pore signature is D/E/E/G in the *Petromyzon* $Na_V2(Ca_V4)$, but in cartilaginous fish and the coelacanth, the pore signature is the common D/E/E/A (Fig. 4b). It had been thought that $Na_V2(Ca_V4)$ was present only in invertebrate animals, but it is now recognized that this channel remains in the vertebrate lineage. On the other hand, we did not find $Na_V2(Ca_V4)$ in the genomes of ray-finned fish or amphibians, which suggests the gene encoding this channel was independently lost from the lineages of ray-finned fish and tetrapods. Considering that both "gene loss" events appear to have occurred as the animals left the sea for inland environments, changes in the ionic conditions may have decreased the selection pressure to keep the $Na_V2(Ca_V4)$ gene. However, since the operational principles of this type of channel are still unclear, this issue remains to be determined.

7 Independent Gene Duplications of Na_V1 in Teleosts and Amniotes

Recent comparative genome analyses indicate that the last common ancestor of ray-finned fish and tetrapods possessed at least four types of Na_V1, each of which was linked to *HoxA-D* clusters (Widmark et al. 2011; Zakon et al. 2011). The genes encoding $Na_V1.1$, 1.2, 1.3, and 1.7 in amniotes, as well as the Na_X shared by therian mammals, emerged from the ancestral gene linked with *HoxD* cluster through a series of gene duplications, probably in the sequence of [(1.3 (1.2, 1.1)) (1.7, X)] (Fig. 5) (Widmark et al. 2011; Zakon et al. 2011). On the other hand, the gene

Fig. 5 (continued) the amphibian frog (*Xenopus tropicalis*), and humans (*Homo sapiens*). $Na_V1.4$ (*magenta*), $Na_V1.6$ (*green*), and $Na_V1.5/1.8/1.9$ (*yellow*) are monophyletic, while NaV1.1/1.2/1.3/1.7 sequences (*blue*) does not form a clade in this tree. The branches of mammalian Na_V1s are marked with darker colors. NCBI accession numbers are indicated in the tree. The *L. oculatus* sequences are obtained from Ensembl (http://www.ensembl.org/Lepisosteus_oculatus/Info/Index), and thus sequence IDs are of UniProt. The bootstrap values over 80 are shown. The tree was constructed using the WAG model on MEGA7 from gap-free 1,183 amino acid positions aligned by MUSCLE program. (**b**) The pore signatures and the regions corresponding to ankyrin-binding motif and the inactivation latch in vertebrate Na_V1s. The species codes and color codes are as used in Figs. 2, 3, and 4

encoding $Na_V1.6$, a neural Na_V1 linked to *HoxC*, apparently experienced no gene duplications and was single throughout amniote evolution (Fig. 5). In mammals, $Na_V1.1$, 1.2, 1.3, and 1.6 are mainly expressed in CNS neurons and contribute to rapid APs, while $Na_V1.1$ and 1.6 are also expressed to some extent in PNS neurons, and $Na_V1.7$ is selectively expressed in PNS neurons (Table 1) (Goldin 2001). This situation implies that the amniote ancestor utilized $Na_V1.7$ (more precisely the mother gene of 1.7 and 1.1/1.2/1.3) in PNS and $Na_V1.6$ in CNS to independently control the excitability of PNS and CNS neurons, respectively. Later, $Na_V1.1$–1.3, derived from a $Na_V1.7$-like ancestral protein, were recruited for the operation of the CNS in amniotes. The diversity of $Na_V1.1$, 1.2, 1.3, and 1.6 (i.e., the CNS subtypes) enabled independent control of their subcellular distributions in individual neurons, since expression of these subtypes in CNS is not only cell type specific but also cellular compartment specific (Hu et al. 2009; Lorincz and Nusser 2010; Zakon et al. 2011). This diversification of these CNS subtypes would have fine-tuned membrane excitabilities among CNS neurons and led to higher level brain performance in ancestral amniotes, which would contribute to forebrain expansion in amniotes (Zakon et al. 2011).

Like $Na_V1.6$, the amniote $Na_V1.4$ linked to *HoxB* was not duplicated and remained single. This subtype has presumably remained to work in the skeletal muscle of amniotes as well as anamniotes (Widmark et al. 2011; Zakon et al. 2011). Other subtypes, $Na_V1.5$, 1.8, and 1.9, are clustered with *HoxA* and were derived via sequential gene duplication, probably in the sequence [1.5 (1.8, 1.9)] (Fig. 5) (Widmark et al. 2011; Zakon et al. 2011). The mammalian (likely all the amniote) $Na_V1.5$ is expressed in the heart (Table 1) (Rogart et al. 1989), as is the $Na_V1.5$ (more precisely the ancestor gene for $Na_V1.5$ and 1.8/1.9) in shark and lungfish (Zakon et al. 2011). The genomes of the lizard *Anolis* and chick *Gallus* contain the genes encoding $Na_V1.8$ and 1.9, as well as 1.5, while that of the frog *Xenopus* does not, suggesting that these innovations occurred with the evolution of amniotes, as in the case of $Na_V1.1/1.2/1.3/1.7$ diversification (Zakon et al. 2011; see also Fig. 5).

It is known that $Na_V1.8$ and $Na_V1.9$ are specialized to work in the nociceptive DRG neurons, a neural crest derivative, in mammals (and likely in all amniotes) (Table 1) (e.g., Lai et al. 2004). The amniote genes encoding $Na_V1.8$ and 1.9 were derived from a $Na_V1.5$-like mother gene and predominantly function for nociception. Unlike other Na_V1s, $Na_V1.8$ and 1.9 show slow activation and inactivation (reviewed in Lai et al. 2004), despite a conserved I-F-M inactivation latch in both isoforms (Fig. 5b). The slow kinetics of $Na_V1.8/1.9$ may favor generation of graded membrane potential changes, which could be linearly related to nociceptive input. In fact, these channels, especially $Na_V1.9$, are expressed in small unmyelinated neurons (Lai et al. 2004), which is consistent with the fact that the ankyrin-binding motif is not well conserved in mammalian $Na_V1.9$ (Fig. 5b). This suggests critical aspects of nociceptive properties were innovations in amniotes. Another possible benefit of using multiple Na_V1s for nociception is that the slow $Na_V1.8$ and 1.9, fast 1.7, and possibly fast 1.5 may make possible special tuning of the propagation speed of nociceptive signals (Lai et al. 2004). This would enable, for example, adjustment for larger body size or constant/high body temperature in

ancestral amniotes. However, answering this question must await testing whether Na_V1s expressed in nociceptive peripheral neurons do in fact function in nociceptive neurons in amniotes other than mammals and also await characterization of nociceptive properties in anamniotes.

This expansion of the Na_V1 gene family in amniotes, and the additional event needed to derive $Na_V1.7$ and Na_X in the therian ancestor, was mediated through tandem gene duplication. This kind of tandem gene duplication was not detected in their neighboring genes nor in the amniote Ca_V genes. Thus "evolution by gene duplication" in this case apparently occurred specifically to Na_V1 family genes of amniotes (Zakon et al. 2011). This diversification pattern is in contrast to what happened in the lineage of ray-finned fish, where another round of whole genome duplication took place in the ancestor of teleosts (e.g., Novak et al. 2006b; Braasch et al. 2016). Indeed, in the zebrafish genome, at least eight genes for Na_V1 isoforms have been identified – *zscn1Laa/ab*, *5Laa/ab*, *8aa/ab*, and *4aa/ab* associated with *HoxDa/b*, *HoxAa/b*, *HoxCa/b*, and *HoxBa/b* clusters, respectively, although the *HoxDb* cluster was lost from teleosts (Novak et al. 2006b; Widmark et al. 2011; Zakon et al. 2011, Won et al. 2012). The mode of gene duplication that took place in teleosts was not specific to genes encoding Na_V1s; it was global and thus distinct from what happened in amniotes. The gene expression pattern analyses of the zebrafish Na_V1 isoforms revealed considerable variation in the expressed isoforms among the CNS, PNS, heart, and skeletal muscles (Novak et al. 2006a; Won et al. 2012). For example, while the zebrafish heart expresses both of the two paralogous $Na_V1.5$ genes (*zscn5Laa* and *ab*), PNS cells from the DRG express only one of the paralogues (*5Laa*) (Novak et al. 2006a; Won et al. 2012). Electrophysiological studies of zebrafish DRG neurons confirmed that a type of Na^+ current is slowly inactivating and recorded from smaller neurons (presumably mediated by the $Na_V1.5$ encoded in *zscn5Laa*), and another Na^+ current is rapidly inactivating and recorded from larger neurons (Won et al. 2012). Given that other fast Na_V1s are also expressed in the DRG (Won et al. 2012), functional diversification of peripheral neurons and differential utilization of fast and slow Na_V1 isoforms may have been established in parallel in teleosts and mammals, although the degree of functional diversification in the DRG neurons (and also in the kinetics of the expressed Na_V1s) appears greater in those of mammals.

A remarkable feature of the amniotes' body is an elaborate forebrain with a large number of neurons. Ancestral amniotes must have developed multiple sensory systems related to their large body size and to terrestrial habitation, which enabled them to utilize complex environmental stimuli for complex motor behaviors (Zakon et al. 2011). "Specific" expansion of the genes encoding Na_V1 isoforms in amniotes, namely, the evolution of $Na_V1.1$–1.3 and 1.8/1.9, provided functional options that supported radiation of amniotes. This may have relieved the limitation on body size and facilitated modal innovations in the sensory system and high-speed signal processing in the CNS, which constituted a morphological and physiological framework preadapted for the evolution of humankind.

8 Concluding Remarks

Along the history of voltage-gated Na^+ channels, one can see repetitive duplication and diversification of functional units. To establish the 24-TM channel family, two rounds of tandem duplication of a Catsper-like 6-TM unit were required to build a polypeptide composed of serially homologous quadruple domains. The unification of the 24-TM segments made possible asymmetric mutation within a single pseudotetraradial channel such that this structure became a unit for further duplication and diversification that gave rise to various types of voltage-gated channels. Na_V channels were established under this molecular evolutionary trend, and the asymmetric pore signatures of Na_V1 (D/E/K/A) and $Na_V2(Ca_V4)$ (D/E/E/A), as well as the asymmetric domains that include the inactivation latch and the ankyrin-binding domain emerged. In the lineage leading to Na_V channels, some of the genes having emerged via duplication were evolutionary dead ends (e.g., Na_V2 paralogues in cnidarians including $Na_V2.5$ with the D/K/E/A pore signature or Na_V1b and 1c in tunicates), while others became the seeds for future duplication and diversification. The repertoire of Na_V-related channels shrank in some animal lineages but grew in others. Loss of the Na_V1 gene in ambulacrarians is an example of the former, while special expansion of Na_V1 in amniotes is an example of the latter; and each is in good accord with their specific evolutionary steps for adaptation. The presence/absence of Na_V and the multiplication of their isoforms led to fundamental modal shifts in the membrane excitability in animal cells. These fundamental changes expanded/restricted the possibilities for physiological and morphological adaptation of animal bodies, extending the limit on body size, increasing the speed of sensory signal processing and locomotion, facilitating predatory life or habitation on land with an elaborate brain. The evolutionary history of Na_Vs reflects well the major steps in the broader evolution of organisms on earth, with the former possibly serving as a motive force for the latter. The involvement of $Na_V2(Ca_V4)$ channels in animal evolution was also touched on here. Several ion channel groups appear to have lost their Ca^{2+} permeability in parallel during the course of vertebrate evolution (Schredelseker et al. 2010; Nishino et al. 2011; Hirai et al. 2017). Further studies of the types of Ca^{2+}-permeable/impermeable Na_V-related channels may provide another key to understanding unknown aspects of cellular and organismal adaptations to their environment.

References

Akopian AN, Sivilotti L, Wood JN (1996) A tetrodotoxin-resistant voltage-gated sodium channel expressed by sensory neurons. Nature 379:257–262

Amemiya CT, Alföldi J, Lee AP, Fan S, Philippe H, Maccallum I, Braasch I, Manousaki T, Schneider I, Rohner N, Organ C, Chalopin D, Smith JJ, Robinson M, Dorrington RA,

Gerdol M, Aken B, Biscotti MA, Barucca M, Baurain D, Berlin AM, Blatch GL, Buonocore F, Burmester T, Campbell MS, Canapa A, Cannon JP, Christoffels A, De Moro G, Edkins AL, Fan L, Fausto AM, Feiner N, Forconi M, Gamieldien J, Gnerre S, Gnirke A, Goldstone JV, Haerty W, Hahn ME, Hesse U, Hoffmann S, Johnson J, Karchner SI, Kuraku S, Lara M, Levin JZ, Litman GW, Mauceli E, Miyake T, Mueller MG, Nelson DR, Nitsche A, Olmo E, Ota T, Pallavicini A, Panji S, Picone B, Ponting CP, Prohaska SJ, Przybylski D, Saha NR, Ravi V, Ribeiro FJ, Sauka-Spengler T, Scapigliati G, Searle SM, Sharpe T, Simakov O, Stadler PF, Stegeman JJ, Sumiyama K, Tabbaa D, Tafer H, Turner-Maier J, van Heusden P, White S, Williams L, Yandell M, Brinkmann H, Volff JN, Tabin CJ, Shubin N, Schartl M, Jaffe DB, Postlethwait JH, Venkatesh B, Di Palma F, Lander ES, Meyer A, Lindblad-Toh K (2013) The African coelacanth genome provides insights into tetrapod evolution. Nature 496:311–316

Anderson PAV, Holman MA, Greenberg RM (1993) Deduced amino acid sequence of a putative sodium channel from the scyphozoan jellyfish *Cyanea capillata*. Proc Natl Acad Sci U S A 90:7419–7423

Beneski DA, Catterall WA (1980) Covalent labeling of protein components of the sodium channel with a photoactivable derivative of scorpion toxin. Proc Natl Acad Sci U S A 77:639–643

Bichet D, Haass FA, Jan LY (2003) Merging functional studies with structures of inward-rectifier K$^+$ channels. Nat Rev Neurosci 4:957–967

Braasch I, Gehrke AR, Smith JJ, Kawasaki K, Manousaki T, Pasquier J, Amores A, Desvignes T, Batzel P, Catchen J, Berlin AM, Campbell MS, Barrell D, Martin KJ, Mulley JF, Ravi V, Lee AP, Nakamura T, Chalopin D, Fan S, Wcisel D, Cañestro C, Sydes J, Beaudry FE, Sun Y, Hertel J, Beam MJ, Fasold M, Ishiyama M, Johnson J, Kehr S, Lara M, Letaw JH, Litman GW, Litman RT, Mikami M, Ota T, Saha NR, Williams L, Stadler PF, Wang H, Taylor JS, Fontenot Q, Ferrara A, Searle SM, Aken B, Yandell M, Schneider I, Yoder JA, Volff JN, Meyer A, Amemiya CT, Venkatesh B, Holland PW, Guiguen Y, Bobe J, Shubin NH, Di Palma F, Alföldi J, Lindblad-Toh K, Postlethwait JH (2016) The spotted gar genome illuminates vertebrate evolution and facilitates human-teleost comparisons. Nat Genet 48:427–437

Brozovic M, Martin C, Dantec C, Dauga D, Mendez M, Simion P, Percher M, Laporte B, Scornavacca C, Di Gregorio A, Fujiwara S, Gineste M, Lowe EK, Piette J, Racioppi C, Ristoratore F, Sasakura Y, Takatori N, Brown TC, Delsuc F, Douzery E, Gissi C, McDougall A, Nishida H, Sawada H, Swalla BJ, Yasuo H, Lemaire P (2016) ANISEED 2015: a digital framework for the comparative developmental biology of ascidians. Nucleic Acids Res 44:D808–D818

Brunet T, Arendt D (2015) From damage response to action potentials: early evolution of neural and contractile modules in stem eukaryotes. Philos Trans R Soc Lond B Biol Sci 371:20150043

Calcraft PJ, Arredouani A, Ruas M, Pan Z, Cheng X, , Hao X, Tang J, Rietdorf K, Teboul L, Chuang K-T, Lin P, Xiao R, Wang C, Zhu Y, Lin Y, Wyatt CN, Parrington J, Ma J, Evans AM, Galione A, Zhu MX (2009) NAADP mobilizes calcium from acidic organelles through two-pore channels. Nature 459:596–600

Catterall WA (2000) From ionic currents to molecular mechanisms: the structure and function of voltage-gated sodium channels. Neuron 26:13–25

Catterall WA, Zheng N (2015) Deciphering voltage-gated Na$^+$ and Ca^{2+} channels by studying prokaryotic ancestors. Trends Biochem Sci 40:526–534

Catterall WA, Goldin AL, Waxman SG (2005) International union of pharmacology. XLVII. Nomenclature and structure-function relationships of voltage-gated sodium channels. Pharmacol Rev 57:397–409

Cavalier-Smith T (2010) Kingdoms Protozoa and Chromista and the eozoan root of the eukaryotic tree. Biol Lett 6:342–345

Conway-Morris S (1986) The community structure of the Middle Cambrian Phyllopod Bed (Burgess Shale). Palaeontology 29:423–467

Delsuc F, Brinkmann H, Chourrout D, Philippe H (2006) Tunicates and not cephalochordates are the closest living relatives of vertebrates. Nature 439:965–968

Fujiu K, Nakayama Y, Yanagisawa A, Sokabe M, Yoshimura K (2009) *Chlamydomonas CAV2* encodes a voltage-dependent calcium channel required for the flagellar waveform conversion. Curr Biol 19:133–139

Fukushima Y (1981) Identification and kinetic properties of the current through a single Na^+ channel. Proc Natl Acad Sci U S A 78:1274–1277

Gans C, Northcutt RG (1983) Neural crest and the origin of vertebrates: a new head. Science 220:268–273

Garrido JJ, Giraud P, Carlier E, Fernandes F, Moussif A, Fache MP, Debanne D, Dargent B (2003) A targeting motif involved in sodium channel clustering at the axon initial segment. Science 300:2091–2094

Gellens ME, George AL Jr, Chen L, Chahine M, Horn R (1992) Primary structure and functional expression of the human cardiac tetrodotoxin-insensitive voltage-dependent sodium channel. Proc Natl Acad Sci U S A 89:554–558

Goldin AL (2001) Resurgence of sodium channel research. Annu Rev Physiol 63:871–894

Gosselin-Badaroudine P, Moreau A, Simard L, Cens T, Rousset M, Collet C, Charnet P, Chahine M (2016) Biophysical characterization of the honeybee DSC1 orthologue reveals a novel voltage-dependent Ca^{2+} channel subfamily: Ca_V4. J Gen Physiol 148:133–145

Gould SJ (1990) Wonderful life: the Burgess Shale and the nature of history. WW Norton & Co., New York

Gur Barzilai M, Reitzel AM, Kraus JE, Gordon D, Technau U, Gurevitz M, Moran Y (2012) Convergent evolution of sodium ion selectivity in metazoan neuronal signaling. Cell Rep 2:242–248

Hartshorne RP, Catterall WA (1981) Purification of the saxitoxin receptor of the sodium channel from rat brain. Proc Natl Acad Sci U S A 78:4620–4624

Hartshorne RP, Keller BU, Talvenheimo JA, Catterall WA, Montal M (1985) Functional reconstitution of the purified brain sodium channel in planar lipid bilayers. Proc Natl Acad Sci U S A 82:240–244

Heinemann SH, Terlau H, Stühmer W, Imoto K, Numa S (1992) Calcium channel characteristics conferred on the sodium channel by single mutations. Nature 356:441–443

Hill AS, Nishino A, Nakajo K, Zhang G, Fineman JR, Selzer ME, Okamura Y, Cooper EC (2008) Ion channel clustering at the axon initial segment and node of Ranvier evolved sequentially in early chordates. PLoS Genet 4:e1000317

Hirai S, Hotta K, Kubo Y, Nishino A, Okabe S, Okamura Y, Okado H (2017) AMPA glutamate receptors are required for sensory-organ formation and morphogenesis in the basal chordate. Proc Natl Acad Sci U S A 114:3939–3944

Hiyama TY, Noda M (2016) Sodium sensing in the subfornical organ and body-fluid homeostasis. Neurosci Res 113:1–11

Hiyama TY, Watanabe E, Ono K, Inenaga K, Tamkun MM, Yoshida S, Noda M (2002) Na_X channel involved in CNS sodium-level sensing. Nat Neurosci 5:511–512

Hiyama TY, Watanabe E, Okado H, Noda M (2004) The subfornical organ is the primary locus of sodium-level sensing by Na_X sodium channels for the control of salt-intake behavior. J Neurosci 24:9276–9281

Hodgkin AL, Huxley AF (1945) Resting and action potentials in single nerve fibers. J Physiol 104:176–195

Hodgkin AL, Huxley AF (1952) Currents carried by sodium and potassium ions through the membrane of the giant axon of *Loligo*. J Physiol 116:449–472

Holland ND (2003) Early central nervous system evolution: an era of skin brains? Nat Rev Neurosci 4:617–627

Holland ND (2016) Nervous systems and scenarios for the invertebrate-to-vertebrate transition. Phil Trans R Soc Lond B 371:20150047

Hong CS, Ganetzky B (1994) Spatial and temporal expression patterns of two sodium channel genes in *Drosophila*. J Neurosci 14:5160–5169

Honoré E (2007) The neuronal background K2P channels: focus on TREK1. Nat Rev Neurosci 8:251–261

Hu W, Tian C, Li T, Yang M, Hou H, Shu Y (2009) Distinct contributions of $Na_V1.6$ and $Na_V1.2$ in action potential initiation and backpropagation. Nat Neurosci 12:996–1002

Hyman LH (1955) The invertebrates: Echinodermata. The coelomic Bilateria. McGraw-Hill, New York

Jiang Y, Lee A, Chen J, Ruta V, Cadene M, Chait BT, MacKinnon R (2003) X-ray structure of a voltage-dependent K^+ channel. Nature 423:33–41

Kole MH, Stuart GJ (2012) Signal processing in the axon initial segment. Neuron 73:235–247

Krebs HA (1975) The August Krogh principle: "For many problems there is an animal on which it can be most conveniently studied". J Exp Zool 194:221–225

Kulkarni NH, Yamamoto AH, Robinson KO, Mackay TFC, Anholt RR (2002) The DSC1 channel, encoded by the *smi60E* locus, contributes to odor-guided behavior in *Drosophila melanogaster*. Genetics 161:1507–1516

Lai J, Porreca F, Hunter JC, Gold MS (2004) Voltage-gated sodium channels and hyperalgesia. Annu Rev Pharmacol Toxicol 44:371–397

Lamaillet G, Walker B, Lambert S (2003) Identification of a conserved ankyrin-binding motif in the family of sodium channel alpha subunits. J Biol Chem 278:27333–27339

Liebeskind BJ, Hillis DM, Zakon HH (2011) Evolution of sodium channels predates the origin of nervous systems in animals. Proc Natl Acad Sci U S A 108:9154–9159

Liebeskind BJ, Hillis DM, Zakon HH (2012) Phylogeny units animal sodium leak channels with fungal calcium channels in an ancient, voltage-insensitive clade. Mol Biol Evol 29:3613–3616

Liebeskind BJ, Hillis DM, Zakon HH (2013) Independent acquisition of sodium selectivity in bacterial and animal sodium channels. Curr Biol 23:R948–R949

Lorincz A, Nusser Z (2010) Molecular identity of dendritic voltage-gated sodium channels. Science 328:906–909

Loughney K, Kreber R, Ganetzky B (1989) Molecular analysis of the *para* locus, a sodium channel gene in *Drosophila*. Cell 58:1143–1154

Lu B, Su Y, Das S, Liu J, Xia J, Ren D (2007) The neuronal channel NALCN contributes resting sodium permeability and is required for normal respiratory rhythm. Cell 129:371–383

Machemer H, Ogura A (1979) Ionic conductances of membranes in ciliated and deciliated *Paramecium*. J Physiol 296:49–60

Moran Y, Zakon HH (2014) The evolution of the four subunits of voltage-gated calcium channels: ancient roots, increasing complexity, and multiple losses. Genome Biol Evol 6:2210–2217

Moran Y, Liebeskind BJ, Zakon HH (2015) Evolution of voltage-gated ion channels at the emergence of Metazoa. J Exp Biol 218:515–525

Murata Y, Iwasaki H, Sasaki M, Inaba K, Okamura Y (2005) Phosphoinositide phosphatase activity coupled to an intrinsic voltage sensor. Nature 435:1239–1243

Nagahora H, Okada T, Yahagi N, Chong JA, Mandel G, Okamura Y (2000) Diversity of voltage-gated sodium channels in the ascidian larval nervous system. Biochem Biophys Res Commun 275:558–564

Nishino A, Baba SA, Okamura Y (2011) A mechanism for graded motor control encoded in the channel properties of the muscle ACh receptor. Proc Natl Acad Sci U S A 108:2599–2604

Noda M, Shimizu S, Tanabe T, Takai T, Kayano T, Ikeda T, Takahashi H, Nakayama H, Kanaoka Y, Minamino N, Kangawa K, Matsuo H, Raftery MA, Hirose T, Inayama S, Hayashida H, Miyata T, Numa S (1984) Primary structure of electrophorus electricus sodium channel deduced from cDNA sequence. Nature 312:121–127

Noda M, Suzuki H, Numa S, Stühmer W (1989) A single point mutation confers tetrodotoxin and saxitoxin insensitivity on the sodium channel II. FEBS Lett 259:213–216

Nomaksteinsky M, Röttinger E, Dufour HD, Chettouh Z, Lowe CJ, Martindale MQ, Brunet JF (2009) Centralization of the deuterostome nervous system predates chordates. Curr Biol 19:1264–1269

Novak AE, Taylor AD, Pineda RH, Lasda EL, Wright MA, Ribera AB (2006a) Embryonic and larval expression of zebrafish voltage-gated sodium channel α-subunit genes. Dev Dyn 235:1962–1973

Novak AE, Jost MC, Lu Y, Taylor AD, Zakon HH, Ribera AB (2006b) Gene duplications and evolution of vertebrate voltage-gated sodium channels. J Mol Evol 63:208–221

Ohno S (1970) Evolution by gene duplication. Springer, New York

Okada T, Hirano H, Takahashi K, Okamura Y (1997) Distinct neuronal lineages of the ascidian embryo revealed by expression of a sodium channel gene. Dev Biol 190:257–272

Okado H, Takahashi K (1988) A simple "neural induction" model with two interacting cleavage-arrested ascidian blastomeres. Proc Natl Acad Sci U S A 85:6197–6201

Okamoto H, Takahashi K, Yamashita N (1977) One-to-one binding of a purified scorpion toxin to Na channels. Nature 266:465–468

Okamura Y, Shidara M (1987) Kinetic differences between Na channels in the egg and the neutrally differentiated blastomere in the tunicate. Proc Natl Acad Sci U S A 84:8702–8706

Okamura Y, Shidara M (1990a) Changes in sodium channels during neural differentiation in the isolated blastomere of the ascidian embryo. J Physiol 431:39–74

Okamura Y, Shidara M (1990b) Inactivation kinetics of the sodium channel in the egg and the isolated, neutrally differentiated blastomere of the ascidian. J Physiol 431:75–102

Okamura Y, Ono F, Okagaki R, Chong JA, Mandel G (1994) Neural expression of a sodium channel gene requires cell-specific interactions. Neuron 13:937–944

Okamura Y, Nishino A, Murata Y, Nakajo K, Iwasaki H, Ohtsuka Y, Tanaka-Kunishima M, Takahashi N, Hara Y, Yoshida T, Nishida M, Okado H, Watari H, Meinertzhagen IA, Satoh N, Takahashi K, Satou Y, Okada Y, Mori Y (2005) Comprehensive analysis of the ascidian genome reveals novel insights into the molecular evolution of ion channel genes. Physiol Genomics 22:269–282

Pan Z, Kao T, Horvath Z, Lemos J, Sul JY, Cranstoun SD, Bennett V, Scherer SS, Cooper EC (2006) A common ankyrin-G-based mechanism retains KCNQ and Na$_V$ channels at electrically active domains of the axon. J Neurosci 26:2599–2613

Parker A (2003) In the blink of an eye. Basic Books, New York

Payandeh J, Minor DL Jr (2015) Bacterial voltage-gated sodium channels (BacNa$_V$s) from the soil, sea, and salt lakes enlighten molecular mechanisms of electrical signaling and pharmacology in the brain and heart. J Mol Biol 427:3–30

Putnam NH, Butts T, Ferrier DE, Furlong RF, Hellsten U, Kawashima T, Robinson-Rechavi M, Shoguchi E, Terry A, Yu JK, Benito-Gutiérrez EL, Dubchak I, Garcia-Fernàndez J, Gibson-Brown JJ, Grigoriev IV, Horton AC, de Jong PJ, Jurka J, Kapitonov VV, Kohara Y, Kuroki Y, Lindquist E, Lucas S, Osoegawa K, Pennacchio LA, Salamov AA, Satou Y, Sauka-Spengler T, Schmutz J, Shin-I T, Toyoda A, Bronner-Fraser M, Fujiyama A, Holland LZ, Holland PW, Satoh N, Rokhsar DS (2008) The amphioxus genome and the evolution of the chordate karyotype. Nature 453:1064–1071

Ramaswami M, Tanouye MA (1989) Two sodium-channel genes in *Drosophila*: implications for channel diversity. Proc Natl Acad Sci U S A 86:2079–2082

Ramsey IS, Moran MM, Chong JA, Clapham DE (2006) A voltage-gated proton-selective channel lacking the pore domain. Nature 440:1213–1216

Ren D, Navarro B, Xu H, Yue L, Shi Q, Clapham DE (2001) A prokaryotic voltage-gated sodium channel. Science 294:2372–2375

Rogart RB, Cribbs LL, Muglia LK, Kephart DD, Kaiser MW (1989) Molecular cloning of a putative tetrodotoxin-resistant rat heart Na$^+$ channel isoform. Proc Natl Acad Sci U S A 86:8170–8174

Roger AJ, Simpson AGB (2008) Evolution: revisiting the root of the eukaryote tree. Curr Biol 19: R165–R167

Rogozin IB, Basu MK, Csürös M, Koonin EV (2009) Analysis of rare genomic changes does not support the unikont-bikont phylogeny and suggests cyanobacterial symbiosis as the point of primary radiation of eukaryotes. Genome Biol Evol 1:99–113

Salkoff L, Butler A, Wei A, Scavarda N, Giffen K, Ifune C, Goodman R, Mandel G (1987) Genomic organization and deduced amino acid sequence of a putative sodium channel gene in *Drosophila*. Science 237:744–749

Sangameswaran L, Fish LM, Koch BD, Rabert DK, Delgado SG, Ilnicka M, Jakeman LB, Novakovic S, Wong K, Sze P, Tzoumaka E, Stewart GR, Herman RC, Chan H, Eglen RM, Hunter JC (1997) A novel tetrodotoxin-sensitive, voltage-gated sodium channel expressed in rat and human dorsal root ganglia. J Biol Chem 272:14805–14809

Sasaki M, Takagi M, Okamura Y (2006) A voltage sensor-domain protein is a voltage-gated proton channel. Science 312:589–592

Sato C, Matsumoto G (1992) Primary structure of squid sodium channel deduced from the complementary DNA sequence. Biochem Biophys Res Commun 186:61–68

Satou Y, Kawashima T, Kohara Y, Satoh N (2003) Large scale EST analyses in *Ciona intestinalis*: its application as northern blot analyses. Dev Genes Evol 213:314–318

Schredelseker J, Shrivastav M, Dayal A, Grabner M (2010) Non-Ca^{2+}-conducting Ca^{2+} channels in fish skeletal muscle excitation-contraction coupling. Proc Natl Acad Sci U S A 107:5658–5663

Shen H, Zhou Q, Pan X, Li Z, Wu J, Yan N (2017) Structure of a eukaryotic voltage-gated sodium channel at near-atomic resolution. Science 355:eaal4326

Smith JJ, Kuraku S, Holt C, Sauka-Spengler T, Jiang N, Campbell MS, Yandell MD, Manousaki T, Meyer A, Bloom OE, Morgan JR, Buxbaum JD, Sachidanandam R, Sims C, Garruss AS, Cook M, Krumlauf R, Wiedemann LM, Sower SA, Decatur WA, Hall JA, Amemiya CT, Saha NR, Buckley KM, Rast JP, Das S, Hirano M, McCurley N, Guo P, Rohner N, Tabin CJ, Piccinelli P, Elgar G, Ruffier M, Aken BL, Searle SM, Muffato M, Pignatelli M, Herrero J, Jones M, Brown CT, Chung-Davidson YW, Nanlohy KG, Libants SV, Yeh CY, McCauley DW, Langeland JA, Pancer Z, Fritzsch B, de Jong PJ, Zhu B, Fulton LL, Theising B, Flicek P, Bronner ME, Warren WC, Clifton SW, Wilson RK, Li W (2013) Sequencing of the sea lamprey (*Petromyzon marinus*) genome provides insights into vertebrate evolution. Nat Genet 45(415–421):421e1–421e2

Strong M, Chandy KG, Gutman GA (1993) Molecular evolution of voltage-sensitive ion channel genes: on the origins of electrical excitability. Mol Biol Evol 10:221–242

Stühmer W, Conti F, Suzuki H, Wang X, Noda M, Yahagi N, Kubo H, Numa S (1989) Structure parts involved in activation and inactivation of the sodium channel. Nature 339:597–603

Takahashi K, Okamura Y (1998) Ion channels and early development of neural cells. Physiol Rev 78:307–337

Takahashi K, Yoshii M (1981) Development of sodium, calcium and potassium channels in the cleavage-arrested embryo of an ascidian. J Physiol 315:515–529

Tate S, Benn S, Hick C, Trezise D (1998) Two sodium channels contribute to the TTX-R sodium current in primary sensory neurons. Nat Neurosci 1:653–655

Tessmar-Raible K, Raible F, Christodoulou F, Guy K, Rembold M, Hausen H, Arendt D (2007) Conserved sensory-neurosecretory cell types in annelid and fish forebrain: insights into hypothalamus evolution. Cell 129:1389–1400

Toledo-Aral JJ, Moss BL, He ZJ, Koszowski AG, Whisenand T, Levinson SR, Wolf JJ, Silos-Santiago I, Halegoua S, Mandel G (1997) Identification of PN1, a predominant voltage-dependent sodium channel expressed principally in peripheral neurons. Proc Natl Acad Sci U S A 94:1527–1532

Tomer R, Denes AS, Tessmar-Raible K, Arendt D (2010) Profiling by image registration reveals common origin of annelid mushroom bodies and vertebrate pallium. Cell 142:800–809

Torruella G, Derelle R, Paps J, Lang BF, Roger AJ, Shalchian-Tabrizi K, Ruiz-Trillo I (2011) Phylogenetic relationships within the Opisthokonta based on phylogenomic analyses of conserved single copy protein domains. Mol Biol Evol 29:531–544

Vergara HM, Bertucci PY, Hantz P, Tosches MA, Achim K, Vopalensky P, Arendt D (2017) Whole-organism cellular gene-expression atlas reveals conserved cell types in the ventral nerve cord of *Platynereis dumerilii*. Proc Natl Acad Sci U S A 114:5878–5885

West JW, Patton DE, Scheuer T, Wang Y, Goldin AL, Catterall WA (1992) A cluster of hydrophobic amino acid residues required for fast Na$^+$-channel inactivation. Proc Natl Acad Sci U S A 89:10910–10914

Widmark J, Sundström G, Ocampo Daza D, Larhammar D (2011) Differential evolution of voltage-gated sodium channels in tetrapods and teleost fishes. Mol Biol Evol 28:859–871

Willey A (1894) Amphioxus and the ancestry of the vertebrates. Macmillan, New York

Won Y-J, Ono F, Ikeda SR (2012) Characterization of Na$^+$ and Ca^{2+} channels in zebrafish dorsal root ganglion neurons. PLoS One 7:e42602

Yan Z, Zhou Q, Wang L, Wu J, Zhao Y, Huang G, Peng W, Shen H, Lei J, Yan N (2017) Structure of the Na$_V$1.4-β1 complex from electric eel. Cell 170:470–482.e11

Yue L, Navarro B, Ren D, Ramos A, Clapham DE (2002) The cation selectivity filter of the bacterial sodium channel, NaChBac. J Gen Physiol 120:845–853

Zakon HH (2012) Adaptive evolution of voltage-gated sodium channels: the first 800 million years. Proc Natl Acad Sci U S A 109(Suppl 1):10619–10625

Zakon HH, Jost MC, Lu Y (2011) Expansion of voltage-dependent Na$^+$ channel gene family in early tetrapods coincided with the emergence of terrestriality and increased brain complexity. Mol Biol Evol 28:1415–1424

Zalc B (2016) The acquisition of myelin: an evolutionary perspective. Brain Res 1641:4–10

Zalc B, Goujet D, Colman D (2008) The origin of the myelination program in vertebrates. Curr Biol 18:R511–R512

Zhang T, Wang Z, Wang L, Luo N, Jiang L, Liu Z, Wu C-F, Dong K (2013) Role of the DSC1 channel in regulating neuronal excitability in *Drosophila melanogaster*: extending nervous system stability under stress. PLoS Genet 9:e1003327

Zhou W, Chung I, Liu Z, Goldin A, Dong K (2004) A voltage-gated calcium-selective channel encoded by a sodium channel-like gene. Neuron 42:101–112